LMI-based reset H∞ analysis and design for linear continuous-time plants

Francesco Fichera, Christophe Prieur, Sophie Tarbouriech, Luca Zaccarian

LMI-based reset $\mathcal{H}_\infty$ analysis and design for linear continuous-time plants

Francesco Fichera, Christophe Prieur, Sophie Tarbouriech and Luca Zaccarian

In this paper, performance analysis for a class of hybrid systems and optimization-based synthesis of a multi-objective reset controller for linear plants are presented. Lyapunov-based conditions to estimate $\mathcal{L}_2$ gain bounds generalizing and relaxing previous results in the literature are provided in an analysis context. In particular, the analysis results allow for growth of the Lyapunov function at jumps, leading to numerically tractable conditions. On the other hand, the synthesis result allows designing via convex tools with a line search a multi-objective reset controller optimizing both the exponential converging rate and the $\mathcal{L}_2$ gain. A novel peculiarity of our scheme is that the underlying linear flow dynamics is not necessarily stabilizing. This last property is the consequence of taking into account in the design where the flowing trajectories lay and leads to improved performance, especially in terms of decay rate. Some simulations illustrate the usefulness of our techniques.

***Index Terms*— $\mathcal{H}_\infty$ performance, Hybrid Lyapunov function, Hybrid control**

I. Introduction

Hybrid dynamical systems are able to represent several dynamical systems coming from different frameworks like, for instance, switching systems, systems with logical modes and impulsive control. In recent years a lot of attention has been focused on feedback control involving a continuous-time plant interconnected with a controller exhibiting switching or resets (namely, hybrid behavior). The architecture of such controllers introduces a flexibility able to overcome some fundamental limitations of linear control (see [3], [17], [19], [30]) and improve the performance of linear systems (see [10]–[12], [32], [33]). In particular, [2], [10], [34] show how introducing resets on the controller state can significantly decrease the $\mathcal{L}_2$ gain between the perturbation and the performance output. Moreover, [12], [33] show how resets may improve the closed-loop performance in terms of overshoot reduction.

Stability analysis of hybrid systems based on Lyapunov conditions is elegantly developed and presented in [16]. Therein, the notion of solution and the fact that Lyapunov functions do not guarantee existence or completeness of solutions is deeply and clearly investigated and explained. Nevertheless, the problem of performance analysis is even more challenging because of the complex behavior that hybrid systems can show. In the context of reset systems, a set of useful results has been given in [29], where Lyapunov-based conditions for verifying $\mathcal{L}_2$ stability for a certain class of hybrid systems are presented, and also [38], where a rigorous study on hybrid control schemes embedding a FORE controller is clearly provided.

Beyond analysis, another fundamental issue studied in recent years concerns the synthesis of a reset controller. In this context, [32], [33] provide convex optimization-based syntheses of a hybrid controller that are also compatible with the control schemes in [12], [13]. Nevertheless, these synthesis strategies assume that the continuous-time map of the reset controller be given, so that only the reset part needs to be designed. Note that this approach of augmenting a given flow map with a hybrid loop in the attempt to achieve stability and/or to improve performance has been widely used in reset control since the FORE architecture (see, for instance, [1], [3], [8]).

The problem of simultaneous design of all the components of a hybrid controller (namely, flow and jump sets and flow and jump maps) is challenging. The main difficulty of this synthesis comes from matching the constraints between the Lyapunov function and the controller architecture, in order to obtain convex conditions. At present, besides the result presented here, whose preliminary results were given in [10], the only other attempt of optimization-based synthesis of an $\mathcal{H}_\infty$ reset controller for a linear plant is in [34]. As compared to the results in [10], here we include all the proofs, we provide previously unpublished analysis tools, and we include a more general construction where the underlying linear continuous-time dynamics (before resets) may be exponentially unstable, while it was constrained to be exponentially stable with the preliminary results in [10].

In this paper, we present both analysis and synthesis results for a reset control architecture inspired by $\mathcal{H}_\infty$ control design. First, we extend the results in [29], providing relaxed Lyapunov-based conditions to estimate an $\mathcal{L}_2$ gain bound for a class of hybrid control systems. Note that this class is wide and includes several works in the literature (notably [12], [13], [27], [37], [38]). Second, we provide convex conditions for simultaneous design of an optimal multi-objective $\mathcal{H}_\infty$ reset controller minimizing the decay rate and minimizing the

Work supported by ANR project LimICOS, contract number 12BS0300501.

F. Fichera, S. Tarbouriech and L. Zaccarian are with CNRS, LAAS, 7 avenue du colonel Roche, F-31400 Toulouse, France and Univ. de Toulouse, LAAS, F-31400 Toulouse, France (email: {ffichera,tarbour,zaccarian}@laas.fr)

L. Zaccarian is also with the Dip. di Ingegneria Industriale, University of Trento, Italy.

C. Prieur is with Department of Automatic Control, Gipsa-lab, Department of Automatic Control, Grenoble Campus, 11 rue des Mathématiques, BP 46, 38402 Saint Martin d'Hères Cedex, France (email: christophe.prieur@gipsa-lab.fr)

$\mathcal{L}_2$ gain for a linear continuous-time plant. The main idea is to combine the reset controller architecture in [12] and the analysis results in this paper by means of a suitable change of coordinates, in order to obtain convex synthesis conditions. As an improvement of our preliminary results of [10], the hybrid controller architecture in this paper allows us to design an $\mathcal{H}_\infty$ reset controller whose flow map is not necessarily stabilizing in the whole state space. This fact, as already noted in [38], enhances the potential of hybrid control, where divergent trajectories, suitably combined by way of resets can characterize stability and fast convergence. We mention that also [34] provides conditions to design a complete $\mathcal{H}_\infty$ reset controller, although the synthesis is single-objective with respect the $\mathcal{L}_2$ gain. However, the way in which the synthesis in [34] guarantees that the trajectories are mapped in the flow set via reset remains unclear.

The paper is structured as follows. Some notations and definitions with references are given next. Section II introduces the class of hybrid systems that we address some of its properties. Moreover, analysis tools to estimate the $\mathcal{L}_2$ gain are presented and compared to the existing ones. In Section III, we recall the hybrid controller architecture and present the main synthesis result. The effectiveness of our technique is shown through simulations, comparatively to linear designs, in Section IV. The proofs of the main results are gathered in Section V to avoid overloading the presentation. Finally some concluding remarks complete the paper.

Notation and preliminaries. Given a vector x, $x^\top$ denotes the transpose of x. The Euclidean norm of a vector is denoted by $|\cdot|$. $\mathbb{R}$ denotes the set of real numbers, $\mathbb{Z}$ denotes the set of integers. Moreover, $\mathbb{R}_{\geq m}$ (respectively, $\mathbb{Z}_{\geq m}$) denotes the set of real numbers larger than or equal to $m \in \mathbb{R}$ (respectively, the set of integers larger than or equal to $m \in \mathbb{Z}$). For a positive integer n, I_n (respectively, 0_n) denotes the identity matrix (respectively, the null matrix) in $\mathbb{R}^{n\times n}$. The subscripts may be omitted when there is no ambiguity. If $\mathcal{A}$ is a compact set, the notation $|x|_{\mathcal{A}} = \min\{|x-y| : y \in \mathcal{A}\}$ indicates the distance of the vector x from the set $\mathcal{A}$. If $\mathcal{A}$ is the origin then $|x|_{\mathcal{A}} = |x|$. Given sets $\mathcal{A} \subset \mathbb{R}^n$ and $\mathcal{B} \subset \mathbb{R}^n$, we say $\mathcal{A} \subset \mathcal{B}$ if $x \in \mathcal{A}$ implies $x \in \mathcal{B}$. For any $s \in \mathbb{R}$, the function $\mathrm{dz} : \mathbb{R} \to \mathbb{R}$ is defined by $\mathrm{dz}(s) = 0$ if $|s| \leq 1$ and $\mathrm{dz}(s) = \mathrm{sgn}(s)(|s|-1)$ if $|s| \geq 1$. A function $\alpha : \mathbb{R}_{\geq 0} \mapsto \mathbb{R}_{\geq 0}$ is a class-$\mathcal{K}_\infty$ function, also written $\alpha \in \mathcal{K}_\infty$, if α is zero at zero, continuous, strictly increasing and unbounded. Given a matrix Q, $\mathrm{He}(Q) = Q+Q^\top$. Moreover, $\lambda_{min}(Q)$ (respectively, $\lambda_{max}(Q)$) denotes the minimum (respectively, the maximum) eigenvalue of Q. The symbol $\otimes$ denotes the Kronecker product [25]. For an introduction of the framework of hybrid systems that is considered in this paper, see the recent works [15], [16]. However, we recall the following definitions that will be useful in the sequel[1].

[1]For a summary of the concepts and the notation used here, the reader is referred to [16], or the summary in [10].

Definition 1:

*i. (**t-decay rate**) Given a hybrid system, a compact set $\mathcal{A} \subset \mathbb{R}^n$ is uniformly globally exponentially stable with t-decay rate $\lambda > 0$ if there exists a strictly positive real number k such that each solution x satisfies*

$$|x(t,j)|_{\mathcal{A}} \leq k\exp(-\lambda t)|x(0,0)|_{\mathcal{A}}, \qquad \forall (t,j) \in \mathrm{dom}(x), \tag{1}$$

where $\mathrm{dom}(x)$ denotes the hybrid time domain of the solution x.

*ii. (t-$\mathcal{L}_2$ **norm of a hybrid signal**) For a hybrid signal w, with domain $\mathrm{dom}(w) \subset \mathbb{R}_{\geq 0} \times \mathbb{Z}_{\geq 0}$, the t-$\mathcal{L}_2$ norm of w is given by*

$$\|w\|_{2t} = \left(\sum_{j \in \mathrm{dom}_j(w)} \int_{t_j}^{t_{j+1}} |w(t,j)|^2 dt \right)^{\frac{1}{2}}, \tag{2}$$

where $\mathrm{dom}_j(w) := \{j \in \mathbb{Z}_{\geq 0} : (t,j) \in \mathrm{dom}(w)$ for some $t \geq 0\}$ and with t_{j+1} possibly being ∞ if $j \in \mathrm{dom}_j(w)$ and $(j+1) \notin \mathrm{dom}_j(w)$.

iii. ($w \in$ t-$\mathcal{L}_2$) For a hybrid signal w, with domain $\mathrm{dom}(w) \subset \mathbb{R}_{\geq 0} \times \mathbb{Z}_{\geq 0}$, we say $w \in$ t-$\mathcal{L}_2$ whenever $\|w\|_{2t} < \infty$. Moreover, for any pair $t_1 \geq t_2$ such that $t_1, t_2 \in \mathrm{dom}_t(w)$, we use $\|w[t_1,t_2]\|_2$ to denote the restriction of (2) to the corresponding subdomain.

$\Diamond$

II. Analysis

A. Analysis problem statement

Consider the hybrid system [3], [13], [29], [36], [38]

$$\begin{cases} \dot{x} &= Ax + Bw \\ \dot{\tau} &= 1 - \mathrm{dz}\left(\frac{\tau}{\rho}\right) \end{cases} \quad (x,\tau) \in \mathcal{C}$$
$$\begin{cases} x^+ &= Gx \\ \tau^+ &= 0 \end{cases} \quad (x,\tau) \in \mathcal{D} \tag{3}$$
$$\begin{aligned} z &= C_z x + D_{zw} w \\ y &= C_p x + D_{pw} w \end{aligned}$$

where $x \in \mathbb{R}^n$ is the ordinary state, $\tau \in \mathbb{R}$ is a dwell-time logic (with $\rho > 0$), $w \in \mathbb{R}^{n_w}$ is an exogenous signal, $z \in \mathbb{R}^{n_z}$ is the performance output, $y \in \mathbb{R}^{n_y}$ is the measured output and $\mathcal{C}$, $\mathcal{D}$ are the flow and jump sets defined, respectively, as

$$\begin{aligned} \mathcal{C} &:= \{(x,\tau) : x \in \mathcal{F} \text{ or } \tau \in [0,\rho]\} \\ &= \{(x,\tau) : x \in \mathcal{F}\} \cup \{(x,\tau) : \tau \in [0,\rho]\}, \end{aligned} \tag{4a}$$
$$\begin{aligned} \mathcal{D} &:= \{(x,\tau) : x \in \mathcal{J} \text{ and } \tau \in [\rho,2\rho]\} \\ &= \{(x,\tau) : x \in \mathcal{J}\} \cap \{(x,\tau) : \tau \in [\rho,2\rho]\}, \end{aligned} \tag{4b}$$

with $\mathcal{F}$ and $\mathcal{J}$ symmetric cones defined by a matrix $M = M^\top \in \mathbb{R}^{n\times n}$ as

$$\mathcal{F} := \left\{x \in \mathbb{R}^n : x^\top M x \leq 0\right\}, \tag{4c}$$
$$\mathcal{J} := \left\{x \in \mathbb{R}^n : x^\top M x \geq 0\right\}. \tag{4d}$$

Note that (3) and $\mathcal{C} \cup \mathcal{D} = \mathbb{R}^n \times [0,2\rho]$ satisfy the Basic Assumptions of [15] so that solutions exist for all initial conditions of $x \in \mathbb{R}^n$ and for all initial values in $[0,2\rho]$

for the dwell time τ. Since $\mathcal{C} \cup \mathcal{D}$ is forward invariant and no finite escape times are possible due to the linear flow map, then it follows that all maximal solutions are complete and we will refer in the paper to asymptotic stability rather than pre-asymptotic stability (see [15] for more details).

Similar to previous works, in this paper we are concerned about the asymptotic behavior of x and not of timer τ. Therefore, we study stability properties of the compact

$$\mathcal{A} = \{0\} \times [0, 2\rho] \subset \mathbb{R}^n \times [0, 2\rho]. \tag{5}$$

According to [16, Theorem 7.21], robustness comes from compactness of the attractor ser $\mathcal{A}$. Thus all the results presented in this paper satisfies the property of robustness.

The dwell time in (3) relies on a deadzone function which guarantees that set $[0, 2\rho]$ is forward invariant for τ. This is important to guarantee the compactness of the attractor set $\mathcal{A}$ in (5) in order to inherit robustness. Moreover, due to the dwell time, each maximal solution $\xi = (x, \tau)$ to (3)-(4) has a hybrid domain $E = \mathrm{dom}(\xi)$ which is unbounded in the ordinary time t direction. More specifically, any two elements (t, j), (s, k) of E with $t > s$ satisfy the *dwell-time condition* (see [7], [16] for details on dwell-time logic):

$$\rho + t - s \geq \rho(j - k). \tag{6}$$

Notice that all the results in this paper still hold with any dwell-time function guaranteeing the properties above and the compactness of set $\mathcal{A}$ in (5).

The hybrid system (3)-(4) is quite general and represents several works in the literature like [10], [12], [13], [27], [37], [38], which justifies the interest of the results presented here.

The next remark states some important features of solutions to hybrid system (3)-(4).

Remark 1: Consider any solution ξ to system (3)-(4) and its jump times t_i, $i \in \mathrm{dom}_j(\xi) \subset \mathbb{Z}_{\geq 0}$. Then:

i. $t_{i+1} - t_i \geq \rho$, for all $i \in \mathbb{Z}_{\geq 1}$. In particular, if $t_{i+1} - t_i > \rho$, $i \in \mathbb{Z}_{\geq 1}$, then $x(t, i) \in \mathcal{F}$ for all $t \in [t_i + \rho, t_{i+1}]$;
ii. in the interval $[t_0, t_1]$, we have $t_1 - t_0 \geq \rho - \tau(0, 0)$ and so it might happen that $t_1 - t_0 < \rho$ (note that this might also imply that $t_1 = t_0 = 0$ if $\tau(0, 0) \geq \rho$). Nevertheless, $x(t, 0) \in \mathcal{F}$ for all $t \in [\max\{0, \rho - \tau(0, 0)\}, t_1]$;
iii. flow may occur in $\mathcal{J}$ due to the dwell-time logic;
iv. whenever $x \in \mathcal{F} \cap \mathcal{J}$ and $\tau \in [\rho, 2\rho]$, the solution may either jump or flow.

$\star$

Due to the dwell time in (3)-(4) (which guarantees condition (6)), the t-decay rate property (1) implies uniform global exponential stability of the x component of (3)-(4) in the hybrid sense [36]. Furthermore, the dwell time is also a fundamental property that justifies the use of ordinary-time $\mathcal{L}_2$ norms defined in (2) (just as in [10], [14], [29]). In particular, whenever the dwell-time condition (6) is satisfied, the definition in (2) essentially corresponds to the continuous-time $\mathcal{L}_2$ norm of the continuous-time signal $t \mapsto \xi_t(t)$ obtained by projecting on the ordinary time the hybrid arc $(t, j) \mapsto \xi(t, j)$. Note that if the hybrid arc ξ only flows, that is $\mathrm{dom}(\xi) = [0, +\infty) \times \{0\}$, then (2) corresponds to the standard continuous-time $\mathcal{L}_2$ norm. Note also that (2) is not a norm because, for example, a solution ξ starting at a nonzero value at $(t, j) = (0, 0)$ and jumping to zero at $(t, j+1) = (0, 1)$ would satisfy $\|\xi\|_{2t} = 0$ (this is not the case for the hybrid norms introduced in [6], [26]). Nevertheless we call it norm throughout the paper due to the intuition that it generalizes the continuous-time norm.

A common performance index for dynamical systems consists in the worst case t-$\mathcal{L}_2$ norm amplification from an input w and a performance output signal z of interest. More precisely, we want to estimate the finite t-$\mathcal{L}_2$ gain of system (3)-(4) as defined next.

Definition 2: Consider the compact set $\mathcal{A}$ in (5)*. System* (3)-(4) *has finite t-$\mathcal{L}_2$ gain from w to z with gain (upper bounded by) $\gamma > 0$, if any solution to* (3)-(4) *starting from $\mathcal{A}$ satisfies*

$$\|z\|_{2t} \leq \gamma \|w\|_{2t}, \tag{7}$$

for all $w \in t$-$\mathcal{L}_2$. $\Diamond$

In this section, we provide sufficient conditions to establish t-$\mathcal{L}_2$ gain performance bounds for system (3)-(4), relying on a Lyapunov function defined only in the x-state space direction. By proceeding similarly to [29], we want to establish if there exists a non-empty set of possible selections of the dwell-time parameter $\rho > 0$ that guarantee global asymptotic stability of set $\mathcal{A}$ in (5) for system (3)-(4) with $w = 0$ and an estimation of the t-$\mathcal{L}_2$ gain from w to z.

The results will be stated first considering a generic Lyapunov function and afterwards considering a quadratic Lyapunov function which leads to a convenient convex linear matrix inequalities-based (LMI-based) formulation. The reason for this approach is that in [38] an example of a stable hybrid systems for which there does not exist a quadratic Lyapunov function has been given, therefore we do anticipate some level of conservativeness in the quadratic (convex) conditions.

B. Lyapunov-based $\mathcal{L}_2$ stability conditions

We are now ready for the following statement which relies on a generic Lyapunov-like function V. The proof is structured in several steps and is reported in Section V-A to ease out the exposition of the main results.

Theorem 1: Consider system (3)-(4) and the following definitions

$$\tilde{\mathcal{F}} = \left\{ x \in \mathbb{R}^n : x^\top \tilde{M} x \leq 0 \right\}, \tag{8}$$

$$\tilde{\mathcal{F}}_\epsilon = \left\{ x \in \mathbb{R}^n : x^\top \tilde{M} x - \epsilon x^\top x \leq 0 \right\}, \tag{9}$$

with $\tilde{M} = \tilde{M}^\top \in \mathbb{R}^{n \times n}$ and $\epsilon > 0$. If there exist a continuously differentiable function $V : \mathbb{R}^n \to \mathbb{R}_{\geq 0}$ such that set $\tilde{\mathcal{F}}_\epsilon$ in (9) satisfies $\mathcal{F} \subset \tilde{\mathcal{F}}_\epsilon$, and positive real scalars a_1, a_2, a_3, a_4, a_5, $\bar{\gamma}$ and a nonnegative scalar $\underline{\rho}$ satisfying

$$a_1 |x|^2 \leq V(x) \leq a_2 |x|^2, \quad \forall x \in \mathbb{R}^n, \tag{10a}$$

$$\langle \nabla V(x), Ax + Bw \rangle + a_3 V(x) + \frac{1}{\bar{\gamma}} z^\top z - \bar{\gamma} w^\top w < 0, \quad \forall x \in \tilde{\mathcal{F}}_\epsilon \setminus \{0\}, \forall w \in \mathbb{R}^{n_w}, \tag{10b}$$

$$V(Gx) \leq \exp(a_3\underline{\rho})V(x), \quad \forall x \in \mathcal{J}, \tag{10c}$$

$$Gx \in \tilde{\mathcal{F}}, \quad \forall x \in \mathcal{J}, \tag{10d}$$

$$\langle \nabla V(x), Ax + Bw \rangle \leq a_4 V(x) + a_5 |x||w|, \quad \forall x \in \mathbb{R}^n, \forall w \in \mathbb{R}^{n_w}, \tag{10e}$$

then for any γ satisfying

$$\gamma \geq \bar{\gamma} \exp\left(\frac{a_3\underline{\rho}}{2}\right), \quad \gamma > \sqrt{2}|D_{zw}|, \tag{11}$$

there exists $\overline{\rho} > 0$ such that for any $\rho \in (\underline{\rho}, \overline{\rho})$:

1) the set $\mathcal{A}$ in (5) is globally asymptotically stable for the hybrid closed-loop system (3)-(4) with $w = 0$;
2) the finite t-$\mathcal{L}_2$ gain from w to z is less than or equal to γ, namely (7) holds for any solution to (3)-(4) from any initial condition $\xi(0,0) = (x(0,0), \tau(0,0)) \in \mathcal{A}$ and with $w \in t$-$\mathcal{L}_2$.

□

Theorem 1 establishes the existence of $\overline{\rho}$. The next remark reports the functions from which the numerical value of $\overline{\rho}$ can be retrieved.

Remark 2: Exact bounds. Similar to [29, Theorem 1], $\overline{\rho}$ is directly obtained from suitable bounds used in Section V-A. In particular, we may define $\rho_1^\star := \varphi_e^{-1}\left(\frac{\epsilon}{|2(\tilde{M}-\epsilon I)A|}\right)$ where $\tilde{M}$ comes from $\tilde{\mathcal{F}}$ in (8) and $\varphi_e(s) := \frac{1}{2|A|}\left(\exp(2|A|s) - 1\right)$ (note that this bound is different from and less conservative than the corresponding bound in [29]), and it is shown in Section V-A that $\overline{\rho} = \rho_1^\star$ guarantees item 1 of Theorem 1. Moreover, selecting $\rho_2^\star$ and $\rho_3^\star$ as

$$\rho_2^\star := \varphi_1^{-1}(\gamma^2 - 2|D_{zw}|^2), \qquad \rho_3^\star := \varphi_2^{-1}\left(\frac{\epsilon}{a_2 \exp(a_3\underline{\rho})}\right) \tag{12a}$$

$$\varphi_1(s) := \kappa_1(s) + \kappa_2(s) + \frac{2|C_z|^2 s}{a_1}(1 + \kappa_1(s) + \kappa_2(s)) \tag{12b}$$

$$\varphi_2(s) := L_1 \frac{s}{a_1}(1 + \kappa_1(s) + \kappa_2(s)) + L_2\sqrt{\frac{s}{a_1}(1 + \kappa_1(s) + \kappa_2(s))} \tag{12c}$$

$$\kappa_1(s) := \exp\left(\frac{\overline{a}_4}{2}s\right)\kappa(s) + \frac{4a_1\overline{a}_4}{\overline{a}_5^2}\kappa^2(s) \tag{12d}$$

$$\kappa_2(s) := \exp\left(\frac{\overline{a}_4}{2}s\right)\kappa(s) + \kappa^2(s) \tag{12e}$$

$$\kappa(s) := \frac{\overline{a}_5}{2}\sqrt{\frac{\exp(\overline{a}_4 s) - 1}{a_1\overline{a}_4}} \tag{12f}$$

$$L_1 := 2|(\tilde{M} - \epsilon I)A|, \qquad L_2 := 2|(\tilde{M} - \epsilon I)B| \tag{12g}$$

$$\overline{a}_4 := a_4 + a_3, \qquad \overline{a}_5 := a_5 \exp(a_3\underline{\rho}) \tag{12h}$$

it is shown in Section V-A that $\overline{\rho} := \min\{\rho_2^\star, \rho_3^\star\}$, satisfies item 2 of Theorem 1. Therefore the choice $\overline{\rho} := \min\{\rho_1^\star, \rho_2^\star, \rho_3^\star\}$ guarantees both items 1 and 2. ⋆

Theorem 1 generalizes the results in [29] by introducing the following novelties:

- the gain D_{zw} was assumed to be zero in [29], [34]. In particular, the second condition in (11) guarantees that the argument of $\varphi_1(\cdot)$ in (12a) is strictly positive and thus it guarantees also that $\overline{\rho}$ is strictly positive. Note that allowing $D_{zw} \neq 0$ is crucial in many relevant $\mathcal{H}$ type of performance goals (such as set-point regulation).
- increase at jumps of the Lyapunov function $x \mapsto V(x)$ is allowed, while it was not allowed in [29], [34]. By selecting a non-zero $\underline{\rho}$ in (10c), we allow growth at jumps balanced by a strengthened decrease during flow, imposed by the term $a_3 P$ in (10b) (see [16, Proposition 3.29]).
- the requirement in [29, Assumption 1] is removed and replaced by the introduction of set $\tilde{\mathcal{F}}$ and its ϵ-inflation, $\tilde{\mathcal{F}}_\epsilon$, in (8) and (9) respectively, which allow more flexibility. Indeed the dwell-time perturbation upon the trajectories (see Remark 1) is addressed through these inflated sets. However in [29], the jumps have to be mapped in the flow set $\mathcal{F}$ (namely, $Gx \in \mathcal{F}$), which is a requirement relaxed here. In particular, Figure 1(a) shows a case for which [29, Theorem 1] cannot be applied. Figure 1(b) instead, shows a possible selection of sets $\tilde{\mathcal{F}}$ and $\tilde{\mathcal{F}}_\epsilon$ so that Theorem 1 can still be applied. Note that the situation of Figure 1(a) is quite common in certain reset control systems where G maps to the boundary of $\mathcal{F}$. Clearly, [29, Assumption 1] is a particular case of Theorem 1 and it can be retrieved by selecting $\tilde{\mathcal{F}} = \mathcal{F}$ (namely, $\tilde{M} = M$). Finally, we notice that $\tilde{\mathcal{F}} \subset \tilde{\mathcal{F}}_\epsilon$ always holds.

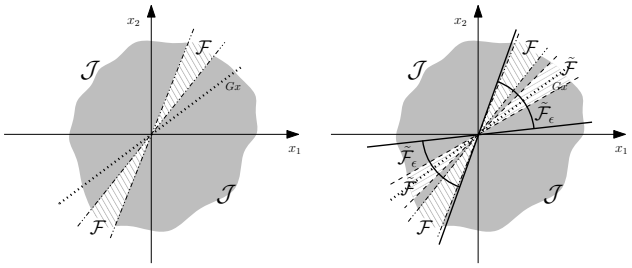

(a) sets $\mathcal{F}$ and $\mathcal{J}$ and jump mapping Gx

(b) $Gx \in \tilde{\mathcal{F}}$ and $\mathcal{F} \subset \tilde{\mathcal{F}}_\epsilon$ (notice also $\tilde{\mathcal{F}} \subset \tilde{\mathcal{F}}_\epsilon$)

Figure 1. Example where [29, Assumption 1] is not satisfied and possible selection of sets $\tilde{F}$ and $\tilde{\mathcal{F}}_\epsilon$ to apply Theorem 1 ($\tilde{\mathcal{F}}$ is the conic region delimited by dashed lines and $\tilde{\mathcal{F}}_\epsilon$ is the conic region delimited by bold lines).

Remark 3: A generic choice of the parameters ϵ and γ in Theorem 1 does not always guarantee that the set of suitable ρ (namely, $(\underline{\rho}, \overline{\rho})$) is non empty. In particular, whenever $\underline{\rho}$ is non-zero (namely, a growth at jumps is admitted) there is no guarantee a priori that $\underline{\rho} < \overline{\rho}$ (see Remark 2). Therefore, whenever $\underline{\rho} > \overline{\rho}$, the set $(\underline{\rho}, \overline{\rho})$ is empty. However, whenever $\underline{\rho} = 0$ (namely no increase at jumps is allowed), since $\rho_1^\star$, $\rho_2^\star$ and $\rho_3^\star$ are strictly positive (see Remark 2), then $\overline{\rho} > 0$ and the set of suitable ρ is $(\underline{\rho}, \overline{\rho}) = (0, \overline{\rho})$ and is non empty. Moreover, we emphasize that $\varphi_e(\cdot)$, $\varphi_1(\cdot)$ and $\varphi_2(\cdot)$ (see Remark 2) are class $\mathcal{K}_\infty$ functions and so also their inverses, which in particular, depend either on γ or on ϵ. Therefore, since $\overline{\rho}$ is the minimum of these last class $\mathcal{K}_\infty$ functions, by enlarging ϵ and/or γ, we may always obtain $\underline{\rho} < \overline{\rho}$. ⋆

Remark 4: There are some special cases for which Theorem 1 can be strengthened:

1. *Global flow condition*: suppose that (10b) holds globally for all $x \in \mathbb{R}^n \setminus \{0\}$ (consider, for instance, the case where $\epsilon \geq \lambda_{max}(\tilde{M})$, namely, $\tilde{\mathcal{F}}_\epsilon = \mathbb{R}^n$). Therefore even when $D_{zw} \neq 0$, the second condition of (11) is not needed and $\gamma = \bar{\gamma}\exp(\frac{a_3\underline{\rho}}{2})$. To see this, it is enough to notice that in the proof of Lemma 1 in Section V, the analysis of Case 1 can be carried out just as in Case 2. Notice that in this case, the set $(\underline{\rho}, \overline{\rho})$ can always be selected as non empty, by arbitrarily enlarging $\overline{\rho}$.
2. *Exponential stability*: item 1 of Theorem 1 establishes global asymptotic stability of set $\{0\} \times [0, 2\rho]$. To prove global *exponential* stability, we should require a further decrease term in (10b). In particular, the term $a_3 V(x)$ in (10b) is needed to compensate for the eventual growth at jumps due to $\underline{\rho}$. Nevertheless, replacing $a_3 V(x)$ in (10b) by $(a_3 + \eta)V(x)$ with $\eta > 0$, then global exponential stability of the attractor $\mathcal{A}$ can be established even when $\underline{\rho} \neq 0$. On the other hand, whenever $\underline{\rho} = 0$, item 1 of Theorem 1 establishes global exponential stability of set $\{0\} \times [0, 2\rho]$, because $a_3 V(x)$ does not have to compensate for any growth at jumps.

$\star$

Notice that whenever $D_{zw} = 0$ and $\underline{\rho} = 0$, then from (11) follows $\gamma = \bar{\gamma}$ retrieving the result in [29].

C. LMI-based $\mathcal{L}_2$ stability conditions

By selecting a quadratic Lyapunov function $V(x) = x^\top P x$, Theorem 1 can be reformulated in the following statement.

Proposition 1: Consider system (3)-(4). If there exist matrices $P = P^\top > 0$, $\tilde{M} = \tilde{M}^\top$, non-negative scalars $\underline{\rho}$, τ_S, τ_F, τ_C, $\tau_R \in \mathbb{R}_{\geq 0}$ and positive scalars ϵ, $\bar{\gamma}$, a_3 such that

$$\begin{pmatrix} A^\top P + PA + a_3 P - \tau_S(\tilde{M} - \epsilon I) & PB & C_z^\top \\ B^\top P & -\bar{\gamma} I & D_{zw}^\top \\ C_z & D_{zw} & -\bar{\gamma} I \end{pmatrix} < 0, \tag{13a}$$

$$G^\top P G - \exp(a_3 \underline{\rho}) P + \tau_R M \leq 0, \tag{13b}$$

$$\tilde{M} - \tau_F M \leq \epsilon I, \tag{13c}$$

$$G^\top \tilde{M} G + \tau_C M \leq 0. \tag{13d}$$

Then for any γ satisfying (11), there exists $\overline{\rho} > 0$ such that for any $\rho \in (\underline{\rho}, \overline{\rho})$:

1) the set $\mathcal{A}$ in (5) is globally exponentially stable for the hybrid closed-loop system (3)-(4), with $w = 0$;
2) the t-$\mathcal{L}_2$ gain from w to z is less than or equal to γ, for all $w \in t$-$\mathcal{L}_2$.

$\square$

Proposition 1 provides a simple tool to solve conditions (10). Indeed conditions (13) are linear except for a_3, τ_S in (13a) and the exponential term in (13b). Therefore to perform the $\mathcal{L}_2$ analysis, a_3 and $\underline{\rho}$ have to be imposed a priori and a line search upon $\tau_S \geq 0$ may to be done. Although this may seem restrictive as compared to the convex results of [29, Theorem 1], the reason why we use the more general formulation of Proposition 1 is to gain important degrees of freedom in the LMI optimization. Indeed practical experience reveals that the conditions in [29, Proposition 1] are prone to numerical problems when looking at situations (such as those of Section III) where some part of the state remains unchanged across jumps. In those cases, allowing for a slight increase of V across jumps results in numerically more tractable conditions. This can be accomplished by fixing small values of $\underline{\rho}$ and a_3 and then solving the arising LMIs condition with a line search on τ_S. This important degree of freedom, which significantly complicates the proof of Theorem 1, was not available in [29]. Moreover [29, Assumption 1] needed to be verified before applying [29, Proposition 1]. Instead in Proposition 1, conditions (13) automatically seek for suitable sets $\tilde{\mathcal{F}}$ and $\tilde{\mathcal{F}}_\epsilon$ satisfying (13) and no further conditions are needed.

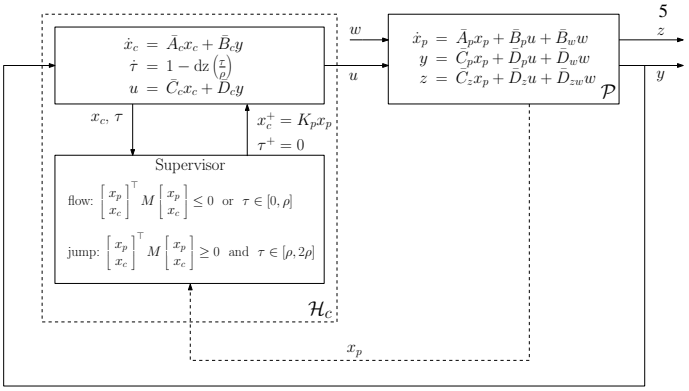

Figure 2. Block diagram of the proposed reset controller.

Remark 5: Simpler cases. In certain cases, conditions (13) can be simplified by solving them with $a_3 = 0$ or $\epsilon = 0$, or both.

i. *Case with* $a_3 = 0$: if $\underline{\rho} = 0$, then a_3 does not need to compensate for any growth at jumps and therefore it can be selected arbitrarily small because of the strict inequality in (13a).
ii. *Case with* $\epsilon = 0$: if $\tau_S = 1$ and $\tilde{M} \leq \tau_F M$ then (13c) holds for any $\epsilon > 0$ and ϵ can be selected arbitrarily small because of the strict inequality in (13a).

Notice that whenever both cases apply, then Proposition 1 recovers the LMI conditions of [29, Proposition 1] and one gets also that set $(\underline{\rho}, \overline{\rho}) = (0, \overline{\rho})$ is always non-empty (see Remark 3). $\star$

III. Synthesis

In this section we propose an optimization-based synthesis method for simultaneous design of flow map, jump map, flow set and jump set of a plant-order reset controller. We will use the results from the previous section and, via a change of

coordinates similar to [10], a convex LMI formulation with a line search will be obtained. The proposed architecture can be well interpreted as a reset version of continuous-time $\mathcal{H}_\infty$ controller synthesis.

A. Synthesis problem statement

According to Figure 2, consider a linear continuous-time plant $\mathcal{P}$, represented by

$$\begin{array}{rcl} \dot{x}_p &=& \bar{A}_p x_p + \bar{B}_p u + \bar{B}_w w \\ z &=& \bar{C}_z x_p + \bar{D}_z u + \bar{D}_{zw} w \\ y &=& \bar{C}_p x_p + \bar{D}_p u + \bar{D}_w w \end{array} \tag{14}$$

where $x_p \in \mathbb{R}^{n_p}$ is the state of the plant, $u \in \mathbb{R}^{n_u}$ is the control input, $y \in \mathbb{R}^{n_y}$ is the measured output (used for the feedback), $w \in \mathbb{R}^{n_w}$ is an exogenous input (comprising disturbances and references) and $z \in \mathbb{R}^{n_z}$ is the performance output.

To keep the presentation simple, we avoid algebraic loops by making the following typical assumption.

Assumption 1: Plant (14) is strictly proper from u to y, namely $\bar{D}_p = 0$. ∘

Note that the previous assumption is not very restrictive. If plant $\mathcal{P}$ has $\bar{D}_p \neq 0$, we can always define $\bar{y} := y - \bar{D}_p u$ and use $\bar{y}$ as a new plant measurement output.

The reset controller architecture $\mathcal{H}_c$ that we propose is given by

$$\begin{array}{l} \left\{ \begin{array}{rcll} \dot{x}_c &=& \bar{A}_c x_c + \bar{B}_c y & \\ \dot{\tau} &=& 1 - \mathrm{dz}\left(\frac{\tau}{\rho}\right) & (x,\tau) \in \mathcal{C}, \\ x_c^+ &=& K_p x_p & \\ \tau^+ &=& 0 & (x,\tau) \in \mathcal{D}, \end{array} \right. \\ u \;=\; \bar{C}_c x_c + \bar{D}_c y, \end{array} \tag{15a}$$

where $x_c \in \mathbb{R}^{n_c}$ and $\tau \in [0, 2\rho]$ is the dwell-time logic and the flow and jump sets $\mathcal{C}$ and $\mathcal{D}$ are defined as in (4a)-(4d). M is a design parameter, and is defined as

$$M := \mathrm{He}\left(PA + \frac{\tilde{\alpha}}{2} P\right), \tag{15b}$$

with A representing the flow map of the closed-loop system (see (3) and also (16)) and $\tilde{\alpha}$, P being controller parameters to be defined. Hybrid controller (15) is the same as the one in [12, Theorem 1], with differences clarified below in Remark 6.

Similar to [10], [31]–[34], we consider state feedback reset laws, namely the jump map and sets $\mathcal{C}$ and $\mathcal{D}$ in (15), depend on the knowledge of the plant state x_p at jump times, which is a strong assumption. Nevertheless, applying the results in [13], whenever the plant state is detectable from y, we may implement the proposed controller in output feedback from y and without a direct measurement of x_p, preserving the closed-loop exponential stability properties established by this design.

The feedback interconnection between $\mathcal{H}_c$ and $\mathcal{P}$ is always possible since Assumption 1 implies well-posedness in the linear sense. Thus, we obtain the hybrid closed-loop system (3)-(4) with $x = [x_p^\top \; x_c^\top]^\top \in \mathbb{R}^{n=n_p+n_c}$ and the selections:

$$\left(\begin{array}{c|c} A & B \\ \hline G & - \\ \hline - & M \\ \hline C_z & D_{zw} \\ \hline C_p & D_{pw} \end{array}\right) = \left(\begin{array}{cc|c} A_p & B_p & B_{pw} \\ B_c & A_c & B_{cw} \\ \hline \multicolumn{2}{c|}{G} & - \\ \hline \multicolumn{2}{c|}{-} & M \\ \hline \multicolumn{2}{c|}{C_z} & D_{zw} \\ \hline \multicolumn{2}{c|}{C_p} & D_{pw} \end{array}\right)$$

$$= \left(\begin{array}{cc|c} \bar{A}_p + \bar{B}_p \bar{D}_c \bar{C}_p & \bar{B}_p \bar{C}_c & \bar{B}_w + \bar{B}_p \bar{D}_c \bar{D}_w \\ \bar{B}_c \bar{C}_p & \bar{A}_c & \bar{B}_c \bar{D}_w \\ \hline I & 0 & - \\ K_p & 0 & - \\ \hline - & - & \mathrm{He}\left(PA + \frac{\tilde{\alpha}}{2} P\right) \\ \hline \bar{C}_z + \bar{D}_z \bar{D}_c \bar{C}_p & \bar{D}_z \bar{C}_c & \bar{D}_{zw} + \bar{D}_z \bar{D}_c \bar{D}_w \\ \hline \bar{C}_p & 0 & \bar{D}_w \end{array}\right). \tag{16}$$

In the sequel, we refer to the interconnection between $\mathcal{H}_c$ and $\mathcal{P}$ as (3)-(4), (16).

Remark 6: As compared to [12], here we want to use the same reset controller architecture to propose a multi-objective simultaneous synthesis optimizing the t-decay rate and the t-$\mathcal{L}_2$ performance introduced in Definition 1. Note that in [12], the proposed optimization-based synthesis for overshoot reduction only concerned the design of the reset loop. In other words for any given flow map (namely, matrix A is given), a solution was proposed to design flow and jump sets and the jump map (namely, M and K_p in (15)) to achieve global exponential stability of the origin, guaranteeing overshoot reduction. However, controller matrices $(\bar{A}_c, \bar{B}_c, \bar{C}_c, \bar{D}_c)$ were not part of the design. Here instead, similar to [10], [34], we propose an optimization-based synthesis to completely design the $\mathcal{H}_\infty$ reset controller, that is, flow and jump maps and flow and jump sets altogether. ⋆

B. Main synthesis results

The following theorem states sufficient conditions for an optimization-based design of the $\mathcal{H}_\infty$ reset controller (15) with respect to the t-decay rate $\tilde{\alpha}$ and the t-$\mathcal{L}_2$ gain γ, introduced in Definition 1. In particular, the theorem provides an almost convex procedure to design a plant-order $\mathcal{H}_\infty$ reset controller. The result is proved by merging the exponential stability results in [12], from which a t-decay rate can be inferred, and the t-$\mathcal{L}_2$ analysis in Proposition 1. In particular, the synthesis is performed without requiring growth at jumps of the Lyapunov function. Thus if $\underline{\rho} = 0$, the set of allowable values of ρ are always non empty and (11) is equivalent to (18) in this particular case. The details of the proof are reported in Section V-B.

Theorem 2: Given plant (14) satisfying Assumption 1 and any set of matrices $Y = Y^\top \in \mathbb{R}^{n_p \times n_p}$, $W = W^\top \in \mathbb{R}^{n_p \times n_p}$, $\hat{A} \in \mathbb{R}^{n_p \times n_p}$, $\hat{B} \in \mathbb{R}^{n_p \times n_y}$, $\hat{C} \in \mathbb{R}^{n_u \times n_p}$, $\hat{D} \in \mathbb{R}^{n_u \times n_y}$,

positive scalars $\bar{\gamma}$, α and a nonnegative scalar $\tau_S \geq 0$ satisfying (19) for some $\tilde{\alpha} \in (0, \alpha]$, select the controller parameters as:

$$
\begin{aligned}
P &= \begin{bmatrix} W & -W \\ -W & W + (Y - W^{-1})^{-1} \end{bmatrix}, \\
K_p &= (Y - W^{-1})Y^{-1}, \\
\bar{D}_c &= \hat{D}, \\
\bar{C}_c &= (\hat{C} - \bar{D}_c \bar{C}_p Y)(Y - W^{-1})^{-1}, \\
\bar{B}_c &= -W^{-1}\hat{B} + \bar{B}_p \bar{D}_c, \\
\bar{A}_c &= -W^{-1}(\hat{A} + W\bar{B}_c\bar{C}_p Y - W\bar{B}_p\bar{C}_c(Y - W^{-1}) \\
&\quad - W(\bar{A}_p + \bar{B}_p\bar{D}_c\bar{C}_p)Y)(Y - W^{-1})^{-1}. \qquad (17)
\end{aligned}
$$

Then, there exists $\overline{\rho} > 0$ such that for any $\rho \in (0, \overline{\rho})$:

- ***t*-decay rate:** the set $\mathcal{A}$ in (5) is globally exponentially stable for the hybrid closed-loop system (3)-(4), (16), with $w = 0$, and the t-decay rate is $\tilde{\alpha}/2$;
- **$\mathcal{H}_\infty$ specification:** for any $w \in t\text{-}\mathcal{L}_2$, the t-$\mathcal{L}_2$ gain from w to z is smaller than or equal to

$$\gamma = \min\{\bar{\gamma}, \sqrt{2}|D_{zw}|\}. \qquad (18)$$

□

$$
\begin{bmatrix} Y & I \\ I & W \end{bmatrix} > 0, \qquad (19a)
$$

$$
\mathrm{He}\left(\bar{A}_p Y + \bar{B}_p \hat{C}\right) + \alpha Y < 0, \qquad (19b)
$$

$$
\mathrm{He}\left(\left[\begin{array}{cc|cc} (1-\tau_S)(\bar{A}_p Y + \bar{B}_p\hat{C}) - \frac{\tau_S\tilde{\alpha}}{2}Y & (1-\tau_S)(\bar{A}_p + \bar{B}_p\hat{D}\bar{C}_p) - \frac{\tau_S\tilde{\alpha}}{2}I & \bar{B}_w + \bar{B}_p\hat{D}\bar{D}_w & 0 \\ (1-\tau_S)\hat{A} - \frac{\tau_S\tilde{\alpha}}{2}I & (1-\tau_S)(W\bar{A}_p + \hat{B}\bar{C}_p) - \frac{\tau_S\tilde{\alpha}}{2}W & W\bar{B}_w + \hat{B}\bar{D}_w & 0 \\ \hline 0 & 0 & -\frac{\bar{\gamma}}{2}I & 0 \\ \bar{C}_z Y + \bar{D}_z\hat{C} & \bar{C}_z + \bar{D}_z\hat{D}\bar{C}_p & \bar{D}_{zw} + \bar{D}_z\hat{D}\bar{D}_w & -\frac{\bar{\gamma}}{2}I \end{array}\right]\right) < 0. \qquad (19c)
$$

Remark 7: Optimization issues. Theorem 2 gives an LMI-based convex procedure with a line-search on $\tau_S \geq 0$ to design an $\mathcal{H}_\infty$ reset controller. Note that the line search must be carried out to get convexity of the optimization. Indeed, (19) becomes an LMI after fixing τ_S. The $(\alpha, \bar{\gamma})$ trade-off in our design can be addressed by fixing $\tilde{\alpha} = \alpha > 0$ and solving an eigenvalue problem minimizing $\bar{\gamma}$. Then the t-decay rate is fixed to be $\tilde{\alpha}/2$ and the t-$\mathcal{L}_2$ gain can be minimized. It may sometimes be desirable to pick $\tilde{\alpha}$ smaller than α to induce longer times between pairs of consecutive resets. ⋆

Remark 8: Line-search effects. Note that (19c) corresponds to (13a) in Proposition 1, and then it is clear that τ_S is the multiplier used in the S-procedure that allows relaxing the flow condition but only enforcing it in $\tilde{\mathcal{F}}_\epsilon$ (see also (10b)). In particular whenever $\tau_S = 0$, the flow set does not appear in (19c) so that, according to Remark 4, item 1, condition (11) (and so the second term in (18)) is not needed, and the t-$\mathcal{L}_2$ gain is $\gamma = \bar{\gamma}$. This is the approach that we followed in our preliminary work [10]. The choice of $\tau_S = 0$ is, however, conservative because in this case (19c) holds for all $x \in \mathbb{R}^n \setminus \{0\}$ and therefore the Lyapunov flow condition holds in all the state space. Whenever $\tau_S > 0$, (19c) holds for all $x \in \tilde{\mathcal{F}}_\epsilon$, so that the fact that trajectories are forced to only flow in $\tilde{\mathcal{F}}_\epsilon$ is taken into account. In this latter case, condition (11) (and so (18)) needs to be satisfied. Furthermore several different scenario can be characterized, according to the value of τ_S in (19c):

- $0 \leq \tau_S < 1$ implies that A in (16) is Hurwitz, namely the linear dynamics before resets is exponentially stable (that is, the flow map of the $\mathcal{H}_\infty$ reset controller stabilizes the continuous-time loop);
- $\tau_S = 1$ implies that A is not necessarily Hurwitz;
- $\tau_S > 1$ implies that A is non Hurwitz and interesting closed-loop responses exhibiting exponentially diverging branches might be observed (see [38]), because the linear dynamics before resets is exponentially unstable.

⋆

The idea behind the proof of Theorem 2 is to combine the results of Proposition 1 and Lemma 2. More precisely, inequalities (19a) and (19c) imply the existence of a matrix $P = \left[\begin{smallmatrix} Y & Z \\ Z & Z \end{smallmatrix}\right]^{-1} = P^\top > 0$ satisfying (13) and then the t-$\mathcal{L}_2$ result follows from Proposition 1. In the meantime, (19a) and (19b) guarantee conditions in Lemma 2, so that the t-decay rate is assessed. Note that we are still using the same Lyapunov function for each objective, and the conservativeness discussed in [35, §IV.A] still holds. However, since the controller state can be reset (this is an extra degree of freedom), better compromises can be obtained in the multi-objective context.

IV. Simulations

In this section we show a few examples applying our results. In particular, we propose a DC motor and a F-8 aircraft. The former example is used to present the advantages of the analysis tools of Section II. The latter example is used to present the advantages of the hybrid multi-objective synthesis. Both examples will be compared to the corresponding linear classical multi-objective case [35].

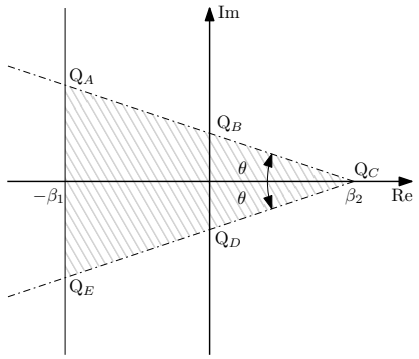

Figure 3. Pole placement region.

In order to avoid fast exponential branches that may damage the actuator or require excessive bandwidth in our control systems, we exploit the advantages of our LMI formulation by adding the following constraints to our syntheses (and also to the corresponding linear designs):

$$-2\beta_1 \otimes X - \mathrm{He}\,(AX) < 0, \tag{20a}$$

$$-2\beta_2 \sin(\theta) \begin{bmatrix} I & 0 \\ 0 & I \end{bmatrix} + \begin{bmatrix} \sin(\theta)I & \cos(\theta)I \\ -\cos(\theta)I & \sin(\theta)I \end{bmatrix} \otimes AX + \begin{bmatrix} \sin(\theta)I & -\cos(\theta)I \\ \cos(\theta)I & \sin(\theta)I \end{bmatrix} \otimes (AX)^\top < 0, \tag{20b}$$

where X and AX in our change of coordinates (see the proof of Theorem 2 in Section V and also [9], [35]) are given by:

$$X := \begin{bmatrix} Y & I \\ I & W \end{bmatrix},\ AX := \begin{bmatrix} \bar{A}_p Y + \bar{B}_p \hat{C} & \bar{A}_p + \bar{B}_p \hat{D} \bar{C}_p \\ \hat{A} & W\bar{A}_p + \hat{B}\bar{C}_p \end{bmatrix},$$

and correspond to the Lyapunov matrix and the closed-loop dynamical matrix, respectively. Enforcing the constraints in (20) guarantees that the poles of the closed-loop feedback (or the continuous-part of the feedback for the reset case) lay in the region pictorially shown in Figure 3. In particular, notice that after the linear synthesis, the poles of the closed-loop feedback will lay in the polygon $\overline{Q_A Q_B Q_C Q_D Q_E}$, because exponential stability is equivalent to having the closed-loop poles in the left-side of the complex plane. The hybrid case is instead nonlinear, thus the synthesis allows for the design of an $\mathcal{H}_\infty$ reset controller whose continuous-time dynamics is not stabilizing. Therefore the poles of the continuous-time part of the reset closed-loop system could be placed anywhere in the complex plane, possibly generating fast positive exponential branches (while stability is induced by resets). In the sequel, we consider $\beta_1 = 50$, $\beta_2 = 25$ and $\theta = \pi/30$ as reasonable values for the systems in exam. All the design is performed by means of *YALMIP* [22].

A. A DC motor

In this example, already used in [10], we want to present the synthesis of a multi-objective $\mathcal{H}_\infty$ reset controller compared to a multi-objective linear $\mathcal{H}_\infty$ controller. Moreover according to [13], we augment the $\mathcal{H}_\infty$ reset controller with an observer in order to have a complete output feedback (where also the resets depend on an estimate of the plant state provided by the observer) and we will use the t-$\mathcal{L}_2$ analysis in Section II to estimate the new t-$\mathcal{L}_2$ gain for the arising hybrid closed loop comprising the $\mathcal{H}_\infty$ reset controller and the observer.

According to (14), let us first introduce the plant:

$$\left[\begin{array}{c|c|c} \bar{A}_p & \bar{B}_p & \bar{B}_w \\ \hline \bar{C}_z & \bar{D}_z & \bar{D}_{zw} \\ \hline \bar{C}_p & \bar{D}_p & \bar{D}_w \end{array}\right] = \left[\begin{array}{cc|c|c} -2.4 & 0 & 2 & 1 \\ 1 & 1 & 0 & 1 \\ \hline 0 & 1 & 10 & 0 \\ \hline 0 & 1 & 0 & 5 \end{array}\right]. \tag{21}$$

The top of Figure 4 shows the t-$\mathcal{L}_2$ gain obtained for the reset and linear case for a given decay-rate α. Similar to [10], the reset controller guarantees lower t-$\mathcal{L}_2$ gains than the linear case, as the the decay-rate increases. Unlike [10], the design strategy in Section III allows us to design an $\mathcal{H}_\infty$ reset controller through a line-search on $\tau_S \geq 0$ (see (19)). The bottom of Figure 4 shows the t-$\mathcal{L}_2$ gains obtained with the hybrid synthesis for $\alpha = 3$ and for $\tau_S \in [0,\ 5]$. Although the t-$\mathcal{L}_2$ gain increases with τ_S, for $\tau_S \geq 1$ we have $\mathcal{H}_\infty$ reset controllers with nonstabilizing continuous-time part (see Remark 8). Indeed, Figure 5(a) shows the behavior of the closed-loop system with the $\mathcal{H}_\infty$ reset controller obtained with $\alpha = \tilde{\alpha} = 3$, $\tau_S = 5$ and $\rho = 5 \cdot 10^{-2}$. Since both the linear and the reset synthesis are designed imposing $\alpha = 3$, we do not have any guarantee that the $\mathcal{H}_\infty$ reset controller leads to faster responses. Nevertheless, the fact that the flow map is unstable requires the action of the reset part to mitigate the unstable modes and to induce exponential stability, with the interesting effects of showing a faster decay rate than the linear case even though the same speed of convergence was imposed by design. In particular according to (15), the synthesis returns the following controller (where M has been

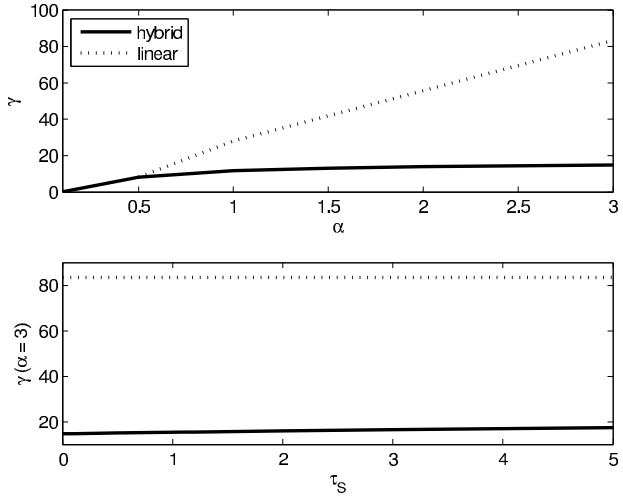

Figure 4. Comparison reset $\mathcal{H}_\infty$ and linear $\mathcal{H}_\infty$ control feedback for the DC motor.

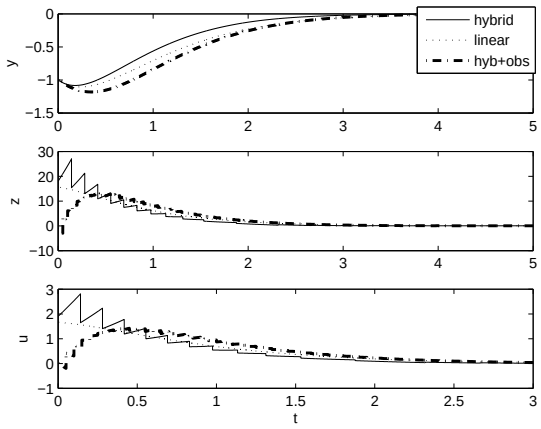

(a) Free response $x_p(0,0) = (-1,\ -1)$ (*i.e.*, $w = 0$)

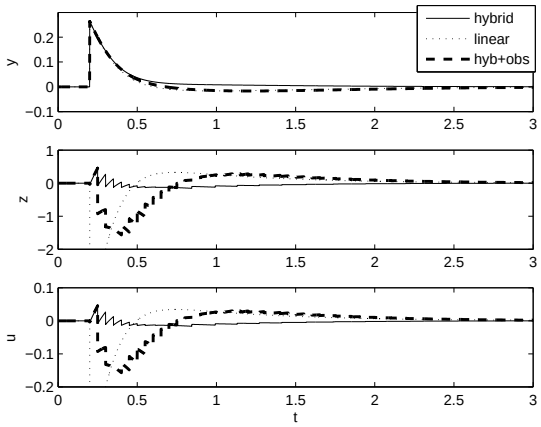

(b) Response with noise $w \in t\text{-}\mathcal{L}_2$.

Figure 5. Simulations for the DC motor, example of Section IV-A.

divided by its determinant)

$$\left[\begin{array}{c|c} \bar{A}_c & \bar{B}_c \\ \hline K_p & - \\ \hline C_c & \bar{D}_c \end{array}\right] = \left[\begin{array}{cc|c} 1.51871 & -1.82471 & 2.17031 \\ 0.89613 & 0.67999 & -0.75037 \\ \hline -0.27132 & -0.87136 & - \\ 0.60395 & 1.41394 & - \\ \hline 1.85009 & 0.11383 & -0.01509 \end{array}\right],$$

$$M = \begin{bmatrix} 0.00579 & 0.01221 & -0.00579 & -0.01221 \\ 0.01221 & 0.02569 & -0.01221 & -0.02569 \\ -0.00579 & -0.01221 & 0.00579 & 0.01221 \\ -0.01221 & -0.02569 & 0.01221 & 0.02569 \end{bmatrix}.$$

Figure 5 contains also the hybrid output feedback case obtained by applying [13, Theorem 1]. The idea is simply to replace x_p by $\hat{x}_p$ in (15) (flow and jump sets included), where $\hat{x}_p$ is the estimated state coming from a classical Luenberger observer [23]:

$$\dot{\hat{x}}_p = (\bar{A}_p - L\bar{C}_p)\hat{x}_p + (\bar{B}_p - L\bar{D}_p)u + Ly, \qquad (22)$$

where the observer gain $L = \left[\begin{smallmatrix} 1.5 & 5.7 \end{smallmatrix}\right]^\top$ has been selected by trial and error.

Notice that the multi-objective nature of the synthesis is lost once the observer is introduced because the t-decay rate is no longer guaranteed. Nevertheless we can use the analysis in Section II to estimate the t-$\mathcal{L}_2$ gain of the new hybrid system. By applying Proposition 1, we use (13) by fixing $a_3 = 1 \cdot 10^{-4}$ and $\underline{\rho} = 1 \cdot 10^{-2}$ and making a line search on τ_S. We obtain that the new t-$\mathcal{L}_2$ gain for the hybrid output feedback is $\gamma = 102.86$ (obtained for $\tau_S = 3$). Clearly, an increase of the t-$\mathcal{L}_2$ gain is to be expected, as compared to the state feedback case, nevertheless through Proposition 1 we are able to still establish an upper bound. Figure 5 shows a desirable behavior of the $\mathcal{H}_\infty$ reset controller, although the case with the observer (bold dashed dot line) is closer to the linear response. The external disturbance w is chosen as $w(t) = \exp(-10t)\sin(2t)$, for all $t \geq 0.2$ and zero otherwise.

B. F-8 plane

Consider now the following MIMO example, used also in [20], representing the longitudinal dynamics of the F-8 aircraft. The system data is

$$\left[\begin{array}{c} \bar{A}_p \\ \hline C_z \\ \hline C_p \end{array}\right] = \left[\begin{array}{ccc|c} -0.8 & -0.0006 & -12 & 0 \\ 0 & -0.014 & -16.64 & -32.2 \\ 1 & -0.0001 & -1.5 & 0 \\ 1 & 0 & 0 & 0 \\ \hline 0 & 0 & 0 & 1 \\ 0 & 0 & -1 & 1 \\ \hline 0 & 0 & 0 & 1 \\ 0 & 0 & -1 & 1 \end{array}\right],$$

$$\left[\begin{array}{c|c} \bar{B}_p & \bar{B}_w \\ \hline \bar{D}_z & \bar{D}_{zw} \\ \hline \bar{D}_p & \bar{D}_w \end{array}\right] = \left[\begin{array}{cc|cc} -19 & -3 & -19 & -3 \\ -0.66 & -0.5 & -0.66 & -0.5 \\ -0.16 & -0.5 & -0.16 & -0.5 \\ 0 & 0 & 0 & 0 \\ \hline 1 & 0 & 0 & 0 \\ 0 & 1 & 0 & 0 \\ \hline 0 & 0 & 0 & 0 \\ 0 & 0 & 0 & 0 \end{array}\right].$$

For the purpose of the simulation, we selected a performance output that penalizes both the control input u and the plant

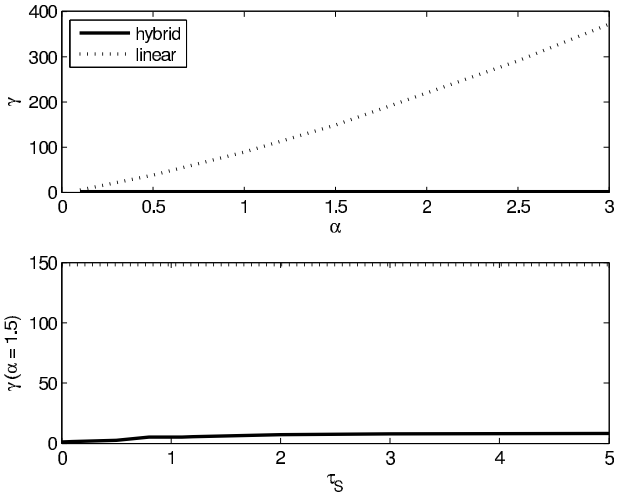

Figure 6. Comparison hybrid and linear control feedback for the F-8.

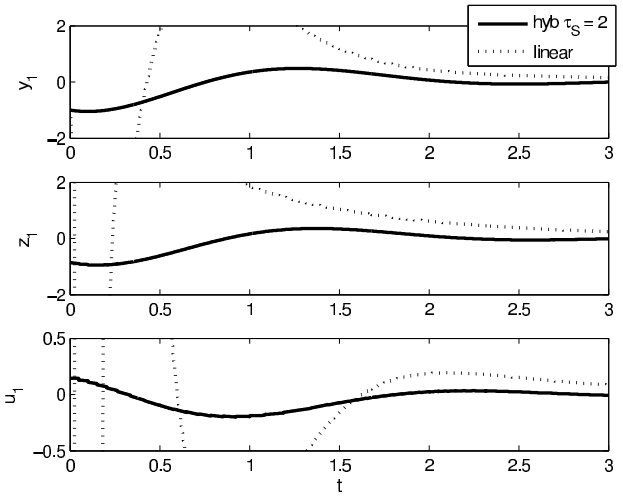

(a) y_1, z_1, u_1

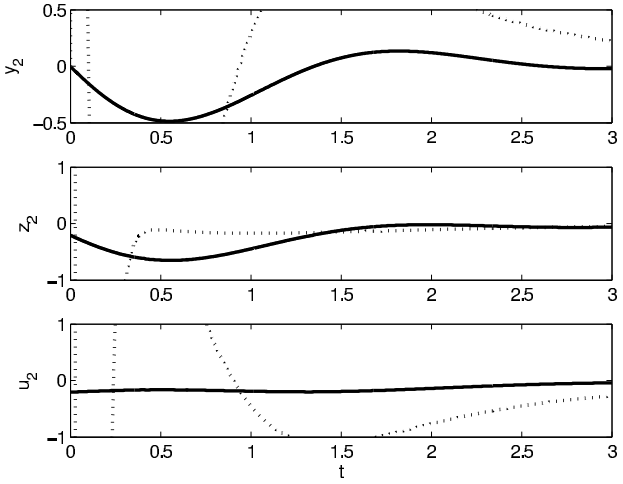

(b) y_2, z_2, u_2

Figure 7. Free response $x_p(0,0) = (-1,\, -1,\, -1,\, -1)$ (*i.e.*, $w = 0$).

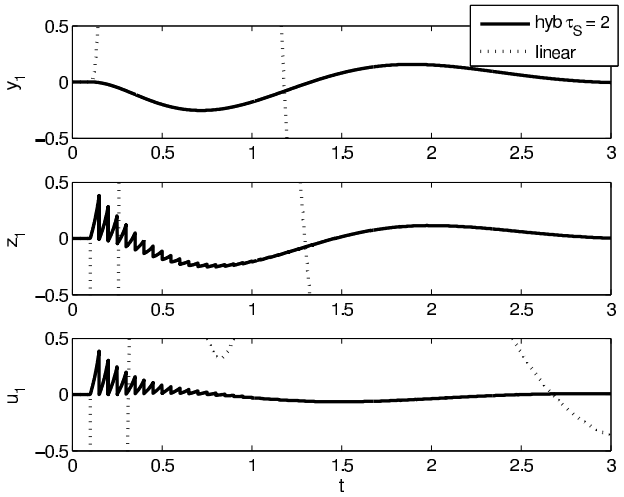

(a) y_1, z_1, u_1

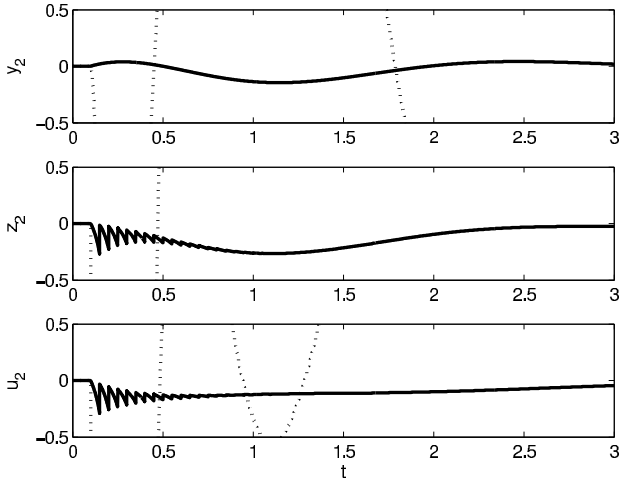

(b) y_2, z_2, u_2

Figure 8. Response with noise $w \in t\text{-}\mathcal{L}_2$.

output y. The top of Figure 6 shows the values of γ obtained with the linear $\mathcal{H}_\infty$ and the reset $\mathcal{H}_\infty$ syntheses as a function of the t-decay rate, and shows that the $\mathcal{H}_\infty$ reset controller induces a certain convergence rate without giving up on the achievable t-$\mathcal{L}_2$ gain, which shows a mild increase. The bottom of Figure 6 shows that for $\alpha = 1.5$, the hybrid synthesis returns $\gamma \simeq 10$ for almost all $\tau_S \geq 0$.

Figures 7 and 8 show the behavior of the $\mathcal{H}_\infty$ reset controller obtained for $\alpha = \tilde{\alpha} = 1.5$ and $\tau_S = 5$. The perturbed case is obtained by using the exogenous signal $w = [w_1\, w_2]^\top$ defined as

$$w_1(t) = \begin{cases} \exp(-10t)\sin(2t) & \text{if } t \geq 2 \\ 0 & \text{if } t < 2 \end{cases},$$

$$w_2(t) = \begin{cases} \exp(-5(t-0.1)) & \text{if } t \geq 0.1 \\ 0 & \text{if } t < 0.1 \end{cases}.$$

We do not report the values of the controller for reason of space. Nevertheless it is easy to see that the controller behaves quite well using much less control than the linear case. In particular, it is possible to see the discontinuous control signal that keeps the trajectories in the flow set guaranteeing a good t-$\mathcal{L}_2$ gain and good t-decay rate due to the unstable nature of the flow map.

V. Proofs and complementary results

A. Proofs of the analysis results

We first introduce the following claim that will be useful in the sequel.

Claim 1: Consider system (3), (4) with $w = 0$ and sets (8) and (9). If (10d) holds then for any $\rho \in (0, \rho_1^\star)$ with $\rho_1^\star := \varphi_e^{-1}\left(\frac{\epsilon}{|2(\tilde{M}-\epsilon I)A|}\right)$, where $\varphi_e(s) := \frac{1}{2|A|}\left(\exp(2|A|s) - 1\right)$, we have

$$x(t_i, i) \in \tilde{\mathcal{F}} \Longrightarrow x(t, i) \in \tilde{\mathcal{F}}_\epsilon, \tag{23}$$

for all $t \in [t_i, t_{i+1}], i \in \mathbb{Z}_{\geq 1}$. ∘

Proof of Claim 1 First recall that $t_{i+1} - t_i \geq \rho$ for all $i \in \mathbb{Z}_{\geq 1}$, due to the dwell time, and in particular $x(t,i) \in \mathcal{F}$ for all $t \in (t_i + \rho, t_{i+1}]$, $i \in \mathbb{Z}_{\geq 1}$ (see also Remark 1). Now similarly

to the proof of [29, Theorem 2], due to the fact that during flow $|\dot{x}| \leq |A||x|$, we have

$$|x(t,i)|^2 \leq \exp(2|A|(t-t_i))|x(t_i,i)|^2,$$

for all $t \in [t_i, t_{i+1}]$, $i \in \mathbb{Z}_{\geq 0}$, which by integrating (differently from [29, Theorem 2]) implies

$$\begin{aligned}\|x[t_i,t]\|_2^2 &\leq \frac{\exp\left(2\,|A|\,(t-t_i)-1\right)}{2\,|A|}|x(t_i,i)|^2 \\ &= \varphi_e(t-t_i)|x(t_i,i)|^2 \end{aligned} \tag{24}$$

for all $t \in [t_i, t_{i+1}]$, $i \in \mathbb{Z}_{\geq 0}$ and $\varphi_e(\cdot)$ defined in the statement[2].

Let us define $\chi(x) := x^\top \tilde{M} x - \epsilon x^\top x$. Thus, we have

$$\langle \nabla \chi, Ax \rangle \leq |2(\tilde{M} - \epsilon I)A||x|^2, \quad \forall x \in \mathbb{R}^n, \tag{25}$$

and due to (10d), $x(t_i,i) \in \tilde{\mathcal{F}}$ for all $i \in \mathbb{Z}_{\geq 1}$, and since $\tilde{\mathcal{F}} \subset \tilde{\mathcal{F}}_\epsilon$, we have

$$\chi(x(t_i,i)) \leq -\epsilon |x(t_i,i)|^2, \quad \forall i \in \mathbb{Z}_{\geq 1}. \tag{26}$$

Then, by integrating (25) and using (24) and (26), for all $t \in [t_i, t_i + \rho]$, $i \in \mathbb{Z}_{\geq 1}$, we have

$$\begin{aligned}\chi(x(t,i)) &\leq \chi(x(t_i,i)) + |2(\tilde{M} - \epsilon I)A|\|x[t_i,t]\|_2^2 \\ &\leq -(\epsilon - \varphi_e(t-t_i)|2(\tilde{M} - \epsilon I)A|)|x(t_i,i)|^2 \\ &< -(\epsilon - \varphi_e(\overline{\rho})|2(\tilde{M} - \epsilon I)A|)|x(t_i,i)|^2 = 0, \end{aligned} \tag{27}$$

where in the last line, we used the fact that $\rho \in (0, \overline{\rho})$ and the definition of $\overline{\rho}$. This concludes the proof of Claim 1. ■

Proof of Theorem 1. First, recall that by definition of (8) and (9), we have that $\tilde{\mathcal{F}} \subset \tilde{\mathcal{F}}_\epsilon$ always holds. Moreover from the statement, we have $\mathcal{F} \subset \tilde{\mathcal{F}}_\epsilon$ and $\xi(0,0) = (x(0,0), \tau(0,0)) \in \{0\} \times [0, 2\rho]$ imply $x(0,0) \in \mathcal{F} \subset \tilde{\mathcal{F}}_\epsilon$. Notice also that due to (10d), we have $x(t_i,i) \in \tilde{\mathcal{F}}$ for all $i \in \mathbb{Z}_{\geq 1}$.

Similarly to [27], define $W(x,\tau) := \varphi(\tau)V(x)$, with $\varphi(\tau) := \exp(a_3 \min\{\tau, \underline{\rho}\})$. Note that for all $\tau \in [0, 2\rho]$, we can write[3]

$$1 \leq \varphi(\tau) \leq \exp(a_3 \underline{\rho}), \tag{28a}$$

$$\dot{\varphi}(\tau) = a_3 \varphi(\tau)\dot{\tau} \leq a_3 \varphi(\tau), \tag{28b}$$

where in the last inequality we used the fact that $\dot{\tau} \leq 1$.

From (10a) and (28a), we have

$$a_1|x|^2 \leq V(x) \leq W(x,\tau) \leq W(x, 2\rho) \leq \exp(a_3\underline{\rho})a_2|x|^2, \tag{29}$$

for all $(x,\tau) \in \mathbb{R}^n \times [0, 2\rho]$.

Consider the variation of W along flow. From (10b) and (28b), we have for all $(x,\tau) \in \tilde{\mathcal{F}}_\epsilon \times [0, 2\rho]$, $x \neq 0$,

$$\begin{aligned}\dot{W}(x,\tau) &= \dot{\varphi}(\tau)V(x) + \varphi(\tau)\dot{V}(x) \\ &< a_3\varphi(\tau)V(x) + \varphi(\tau)(-a_3 V(x) - \frac{1}{\bar{\gamma}} z^\top z + \bar{\gamma} w^\top w) \\ &\leq -\frac{1}{\bar{\gamma}} z^\top z + \bar{\gamma}\exp(a_3\underline{\rho}) w^\top w, \end{aligned} \tag{30}$$

which implies $\dot{W}(x,\tau) < 0$, for all $(x,\tau) \in \tilde{\mathcal{F}}_\epsilon \times [0, 2\rho]$, $x \neq 0$ and $w = 0$.

Consider now the variation of W across jumps. From (10c) and (28a), we have for all $(x,\tau) \in \mathcal{J} \times [\rho, 2\rho]$, $x \neq 0$,

$$\begin{aligned}\Delta W(x,\tau) &= W(Gx, 0) - W(x,\tau) \\ &= V(Gx) - \varphi(\tau)V(x) \\ &\leq (\exp(a_3\underline{\rho}) - \exp(a_3\underline{\rho}))V(x) = 0, \end{aligned} \tag{31}$$

where in the last line we used (28a) and the fact that $\rho > \underline{\rho}$ and that jumps occur only if $\tau \in [\rho, 2\rho]$, namely only when $\varphi(\tau) = \exp(a_3\underline{\rho})$.

Let us now prove item 1 and notice that $\mathcal{F} \subset \tilde{\mathcal{F}}_\epsilon$. From (10d) we have $x(t_i,i) \in \tilde{\mathcal{F}}$ for all $i \in \mathbb{Z}_{\geq 1}$, moreover by applying Claim 1 (namely (23)) and from (30), we get

$$\dot{W}(x(t,i), \tau(t,i)) < 0, \tag{32}$$

for all $t \in [t_i, t_{i+1}]$, $i \in \mathbb{Z}_{\geq 1}$ and $x(t,i) \neq 0$, whenever $\rho \in (0, \rho_1^\star)$ with $\rho_1^\star$ defined in Remark 2 and coming directly from Claim 1. Moreover for all $t \in [t_0, t_1]$, we have two subcases: i. $t \in [t_0, t_0 + \rho]$ and ii. $t \in (t_0 + \rho, t_1]$.

Consider **Case i**. From (28b) and (10e), we have

$$\begin{aligned}\dot{W}(x,\tau) &= \dot{\varphi}(\tau)V(x) + \varphi(\tau)\dot{V}(x) \\ &\leq a_3\varphi(\tau)V(x) + a_4\varphi(\tau)V(x) \\ &= (a_3 + a_4)\varphi(\tau)V(x) \\ &= (a_3 + a_4)W(x,\tau), \end{aligned} \tag{33}$$

for all $(x,\tau) \in \mathbb{R}^n \times [0, 2\rho]$. Therefore for all $t \in [t_i, t_{i+1}]$, $i \in \mathbb{Z}_{\geq 0}$, we get

$$W(x(t,i),\tau(t,i)) \leq \exp((a_3+a_4)(t-t_i))W(x(t_i,i),\tau(t_i,i)), \tag{34}$$

which returns

$$W(x(t,0),\tau(t,0)) \leq \exp((a_3+a_4)\rho)W(x(t_0,0),\tau(t_0,0)), \tag{35}$$

for all $t \in [t_0, t_0 + \rho]$.

Consider **Case ii**. By Remark 1 item ii, we have $x(t,0) \in \mathcal{F} \subset \tilde{\mathcal{F}}_\epsilon$ for all $t \in (t_0 + \rho, t_1]$, therefore also (32) holds for all $t \in (t_0 + \rho, t_1]$.

Therefore by combining (31), (32) and (35), for any initial condition, function $(t,i) \mapsto W(x(t,i),\tau(t,i))$ might grow only in the interval $t \in [t_0, t_0 + \rho]$, and it is strictly decreasing along flow and not increasing at jumps. Recalling that after each jump the system flows yields the result in item 1 of Theorem 1.

To prove item 2, we use the following lemma, which is a generalization of [29, Lemma 1] and whose proof is reported next.

Lemma 1: Consider the definitions in Remark 2 and suppose that the conditions in Theorem 1 hold. Then for any γ in (11),

[2]Notice that for the trivial (and not very interesting) case of a single integrator, we have $|A| = 0$ and the technical proof has to be slightly modified in order to remove a division by zero. In particular, we have $|x(t,i)|^2 = |x(t_i,i)|^2$ and (24) holds with $\varphi_e(t-t_i) := (t-t_i)$.

[3]Due to the definition of φ we should use the generalized gradient as in [27]. Nevertheless to keep the proof simple and without loss of generality we do not use such an expedient, but we consider only the upper bound of $\dot{\varphi}(\tau)$ as in (28b).

there exists $\overline{\rho} > 0$ such that for all $\rho \in (\underline{\rho}, \overline{\rho})$, we have that if $x(t_i, i) \in \tilde{\mathcal{F}}$ and $w \in t\text{-}\mathcal{L}_2$. Moreover, for all $t \in [t_i, t_{i+1}]$, $i \in \mathbb{Z}_{\geq 0}$,

$$\int_{t_i}^{t} |z(s,i)|^2 ds \leq W(x(t_i,i),\tau(t_i,i)) - W(x(t,i),\tau(t,i)) + \gamma^2 \int_{t_i}^{t} |w(s,i)|^2 ds, \tag{36}$$

with $W(x,\tau) := \varphi(\tau)V(x)$ and $\varphi(\tau) := \exp(a_3 \min\{\tau, \underline{\rho}\})$. $\Diamond$

Consider any solution ξ to (3), (4) starting from $\xi(0,0) \in \{0\} \times [0, 2\rho]$. For each $(t,j) \in \mathrm{dom}(\xi)$, denote $t_0 = 0$ and $t_{j+1} = t$. Then using (31) and (36), we have

$$\begin{aligned}
\|z\|_{2t}^2 &= \sum_{i=0}^{j} \int_{t_i}^{t_{i+1}} |z(s,i)|^2 ds \\
&\leq \sum_{i=0}^{j} (W(x(t_i,i),\tau(t_i,i)) - W(x(t_{i+1},i),\tau(t_{i+1},i)) \\
&\qquad + \gamma^2 \|w[t_i, t_{i+1}]\|_2^2) \\
&\leq W(x(t_0,0),\tau(t_0,0)) - W(x(t_{j+1},j),\tau(t_{j+1},j)) \\
&\qquad + \gamma^2 \sum_{i=0}^{j} \|w[t_i,t_{i+1}]\|_2^2 \\
&= -W(x(t,j),\tau(t,j)) + \gamma^2 \|w[t_0,t]\|_2^2 \\
&\leq \gamma^2 \|w\|_{2t}^2,
\end{aligned}$$

for all $(t,j) \in \mathrm{dom}(\xi)$ with $x(t_0,0) = 0$. This completes the proof of item 2, therefore of Theorem 1. ■

Proof of Lemma 1. The proof closely relies on the calculations in the proof of [29, Lemma 1]. Therefore we emphasize here only the different steps.

First, by definition of z in (3), we have

$$\begin{aligned}
|z|^2 &\leq (|C_z||x| + |D_{zw}||w|)^2 \\
&\leq 2|C_z|^2|x|^2 + 2|D_{zw}|^2|w|^2.
\end{aligned} \tag{37}$$

Notice also that from (10e), we can write

$$\begin{aligned}
\langle \nabla V(x), Ax + Bw \rangle &\leq a_4 V(x) + a_5 |x||w| \\
&= (a_4 + a_3)V(x) + a_5|x||w| - a_3 V(x) \\
&:= (\overline{a}_4 - a_3)V(x) + a_5|x||w|, \quad \forall x \in \mathbb{R}^n.
\end{aligned} \tag{38}$$

Therefore from (28a) and (38), we get

$$\begin{aligned}
\dot{W}(x,\tau) &= \dot{\varphi}(\tau)V(x) + \varphi(\tau)\dot{V}(x) \\
&\leq a_3 \varphi(\tau)V(x) + \varphi(\tau)((\overline{a}_4 - a_3)V(x) + a_5|x||w|) \\
&\leq \overline{a}_4 W(x,\tau) + \exp(a_3\underline{\rho}) a_5 |x||w| \\
&:= \overline{a}_4 W(x,\tau) + \overline{a}_5 |x||w|.
\end{aligned} \tag{39}$$

Now, following the same steps as in the proof of [29, Lemma 1], we consider two cases: $t \in [t_i, t_i + \rho]$ and $t \in (t_i + \rho, t_{i+1}]$, with $\rho \in (\underline{\rho}, \overline{\rho})$, $\overline{\rho} := \min\{\rho_2^\star, \rho_3^\star\}$ and $\rho_2^\star$ and $\rho_3^\star$ defined in Remark 2.

Case 1: suppose that $t \in [t_i, t_i + \rho]$. From (29), (39) and using exactly the same calculations as in [29, Lemma 1] we get,

$$\begin{aligned}
W(x(t,i),\tau(t,i)) \leq (1 + &\kappa_1(t - t_i)) W(x(t_i,i),\tau(t_i,i)) \\
&+ \kappa_2(t - t_i)\|w[t_i,t]\|_2^2,
\end{aligned} \tag{40}$$

which is similar to the one in [29, eq. (29)] with $\kappa_1(\cdot)$ and $\kappa_2(\cdot)$ defined in (12). By using (29), (37) and (40), we have

$$\begin{aligned}
|z(t,i)|^2 \leq \frac{2|C_z|^2}{a_1} &((1 + \kappa_1(t - t_i))W(x(t_i,i),\tau(t_i,i)) \\
&+ \kappa_2(t - t_i)\|w[t_i,t]\|_2^2) + 2|D_{zw}|^2 |w(t,i)|^2.
\end{aligned} \tag{41}$$

Note that $\kappa_1(s)$ and $\kappa_2(s)$ are non-decreasing functions, hence we can integrate (41) in the following way

$$\begin{aligned}
&\int_{t_i}^{t} |z(s,i)|^2 ds \\
&\quad \leq \frac{2|C_z|^2(t - t_i)}{a_1} ((1 + \kappa_1(t - t_i))W(x(t_i,i),\tau(t_i,i)) \\
&\qquad + \kappa_2(t - t_i)\|w[t_i,t]\|_2^2) + 2|D_{zw}|^2 \int_{t_i}^{t} |w(s,i)|^2 ds \\
&\quad = \frac{2|C_z|^2(t - t_i)}{a_1} ((1 + \kappa_1(t - t_i))W(x(t_i,i),\tau(t_i,i)) \\
&\qquad + \kappa_2(t - t_i)\|w[t_i,t]\|_2^2) + 2|D_{zw}|^2 \|w[t_i,t]\|_2^2.
\end{aligned} \tag{42}$$

Since we are considering the case where $t - t_i \leq \rho$ and both expressions in (40) and (42) are non-decreasing, we can write

$$\begin{aligned}
W(x(t,i),\tau(t,i)) &\leq (1 + \kappa_1(\rho))W(x(t_i,i),\tau(t_i,i)) \\
&\qquad + \kappa_2(\rho)\|w[t_i,t]\|_2^2,
\end{aligned} \tag{43a}$$

$$\begin{aligned}
\int_{t_i}^{t} |z(s,i)|^2 ds &\leq \frac{2|C_z|^2\rho}{a_1}(1 + \kappa_1(\rho))W(x(t_i,i),\tau(t_i,i)) \\
&\qquad + \left(\frac{2|C_z|^2\rho}{a_1}\kappa_2(\rho) + 2|D_{zw}|^2\right)\|w[t_i,t]\|_2^2,
\end{aligned} \tag{43b}$$

which are similar to [29, eqs. (31)].

Now, we distinguish two subcases: **A.** $\|w[t_i,t]\|_2^2 \geq W(x(t_i,i),\tau(t_i,i))$ and **B.** $\|w[t_i,t]\|_2^2 \leq W(x(t_i,i),\tau(t_i,i))$.

Subcase A: by proceeding with the same calculations as in the proof of [29, Lemma 1], we add and subtract $\frac{2|C_z|^2\rho}{a_1}(1 + \kappa_1(\rho))W(x(t_i,i),\tau(t_i,i))$ to the right hand side of (43a), rearrange and combine with (43b) to get

$$\begin{aligned}
\int_{t_i}^{t} |z(s,i)|^2 ds &\leq W(x(t_i,i),\tau(t_i,i)) - W(x(t,i),\tau(t,i)) \\
&\quad + \Bigg(\kappa_1(\rho) + \kappa_2(\rho) + \frac{2|C_z|^2\rho(1 + \kappa_1(\rho) + \kappa_2(\rho))}{a_1} \\
&\qquad + 2|D_{zw}|^2\Bigg)\|w[t_i,t]\|_2^2 \\
&= W(x(t_i,i),\tau(t_i,i)) - W(x(t,i),\tau(t,i)) \\
&\quad + (\varphi_1(\rho) + 2|D_{zw}|^2)\|w[t_i,t]\|_2^2 \\
&< W(x(t_i,i),\tau(t_i,i)) - W(x(t,i),\tau(t,i))
\end{aligned}$$

$$
\begin{aligned}
&+ (\varphi_1(\rho_2^\star) + 2|D_{zw}|^2)\|w[t_i,t]\|_2^2 \\
&= W(x(t_i,i),\tau(t_i,i)) - W(x(t,i),\tau(t,i)) \\
&\quad + \gamma^2\|w[t_i,t]\|_2^2, \qquad (44)
\end{aligned}
$$

where we used the fact that $\rho < \rho_2^\star$ and in the last line we applied the definition of $\rho_2^\star$ in (12a).

Subcase B: follows exactly the same calculations as in the proof of [29, eqs. (35)-(39)] with respect to the set $\tilde{\mathcal{F}}_\epsilon$. In particular, the fact that $x(t_i,i) \in \tilde{\mathcal{F}}$ implies that $x(t,i) \in \tilde{\mathcal{F}}_\epsilon$ for all $t \in [t_i, t_i+\rho]$ with $\rho < \rho_3^\star$. Therefore since $\mathcal{F} \subset \tilde{\mathcal{F}}_\epsilon$, by integrating (30), we get

$$
\begin{aligned}
\int_{t_i}^{t} |z(s,i|^2 ds &\le W(x(t_i,i),\tau(t_i,i)) - W(x(t,i),\tau(t,i)) \\
&+ \bar{\gamma}^2 \exp(a_3\underline{\rho}) \int_{t_i}^{t} |w(s,i)|^2 ds, \qquad (45)
\end{aligned}
$$

for all $t \in [t_i, t_i+\rho]$. This completes Case 1.

Case 2: suppose that $t \in [t_i+\rho, t_{i+1}]$. Indeed, in the exact same way as in [29, eq. (40)], if $t_{i+1} - t_i > \rho$, then $x(t,i) \in \mathcal{F} \subset \tilde{\mathcal{F}}_\epsilon$ for all $t \in [t_i+\rho, t_{i+1}]$ by definition of the flow set. Therefore, by integrating (30) as above, we get (45) for all $t \in [t_i+\rho, t_{i+1}]$. This completes the proof of Lemma 1. ■

Proof of Proposition 1. The proof is carried out by showing that (13) implies all the conditions in Theorem 1 with a continuously differentiable Lyapunov function $V(x) = x^\top P x$, with $P = P^\top > 0$.

First note that (10a) holds with $a_1 = \lambda_{min}(P)$, $a_2 = \lambda_{max}(P)$ and (10e) follows from $\nabla V(x) = 2Px$, selecting large enough a_4 and a_5. Moreover, by applying the S-procedure (see [4]), (13c) implies $x^\top(\tilde{M} - \epsilon I)x \le 0$ for all x such that $x^\top M x \le 0$, namely $\mathcal{F} \subset \tilde{\mathcal{F}}_\epsilon$ as required by Theorem 1. Recall that $\tilde{\mathcal{F}} \subset \tilde{\mathcal{F}}_\epsilon$ by definition.

Consider now (13a). Indeed, due to the strict inequality in (13a) and the quadratic function V (see [21, Lemma 4.3]), there always exists a small enough $\eta > 0$ such that, by applying a Schur complement [4], we obtain

$$
\begin{aligned}
&\begin{bmatrix} A^\top P + PA + a_3 P - \tau_S(\tilde{M} - \epsilon I) + \eta I & PB \\ B^\top P & 0 \end{bmatrix} \\
&\quad + \begin{bmatrix} C_z & D_{zw} \\ 0 & I \end{bmatrix}^\top \begin{bmatrix} \frac{1}{\bar{\gamma}} I & 0 \\ 0 & -\bar{\gamma} I \end{bmatrix} \begin{bmatrix} C_z & D_{zw} \\ 0 & I \end{bmatrix} < 0. \qquad (46)
\end{aligned}
$$

By pre- and post-multiplying (46) by $\begin{bmatrix} x^\top & w^\top \end{bmatrix}$ and its transpose, respectively, and using the definition of z in (3), we have

$$
\begin{aligned}
&\langle \nabla V(x), Ax + Bw \rangle + a_3 P + \eta |x|^2 \\
&+ \begin{bmatrix} z \\ w \end{bmatrix}^\top \begin{bmatrix} \frac{1}{\bar{\gamma}} I & 0 \\ 0 & -\bar{\gamma} I \end{bmatrix} \begin{bmatrix} z \\ w \end{bmatrix} - \tau_S x^\top (\tilde{M} - \epsilon I) x < 0, \qquad (47)
\end{aligned}
$$

which, by applying S-procedure, implies (10b) with a further decreasing term $\eta > 0$ (see item 2 of Remark 4).

Consider (13b). By pre- and post-multiplying by $x^\top$ and its transpose, respectively, we get $V(Gx) \le \exp(a_3\underline{\rho}) V(x) - \tau_R x^\top M x$, which applying the S-procedure implies (10c).

Finally, consider (13d). In particular by applying S-procedure, (13d) is equivalent to

$$
x^\top G^\top \tilde{M} G x \le 0, \quad \forall x \in \mathcal{J},
$$

which is equivalent to (10d). This completes the proof of Proposition 1. ■

B. Proofs of the synthesis results

The next lemma is useful for the proof of Theorem 2 and is a straightforward generalization of [12, Theorem 1].

Lemma 2: Consider plant (14) under Assumption 1, the reset controller (15) and their interconnection (3)-(4), (16). If there exists a matrix $P = P^\top = \begin{bmatrix} P_p & P_{pc} \\ P_{pc}^\top & P_c \end{bmatrix} > 0$ such that

$$
\begin{aligned}
&\mathrm{He}\left(\bar{P}_p(A_p + B_p K_p) + \frac{\alpha}{2}\bar{P}_p\right) < 0, \qquad (48a) \\
&\bar{P}_p = P_p - P_{pc}P_c^{-1}P_{pc}^\top > 0, \qquad K_p = -P_c^{-1}P_{pc}^\top, \qquad (48b)
\end{aligned}
$$

for some $\alpha > 0$, then for any $\tilde{\alpha} \in (0, \alpha]$ there exists $\overline{\rho} > 0$ such that for all $\rho \in (0, \overline{\rho})$, the Lyapunov function $x \mapsto V(x) = x^\top P x$ satisfies the following properties:

$$
\begin{aligned}
&\Delta V(x) \le 0, \quad \forall x \in \mathbb{R}^n, \qquad (49a) \\
&Gx \in \tilde{F} \subset \mathcal{F}, \quad \forall x \in \mathbb{R}^n, \qquad (49b)
\end{aligned}
$$

where $\tilde{\mathcal{F}} := \{x : x^\top(M + \epsilon I)x \le 0\}$, with M in (15b) (and defining set $\mathcal{F}$), $\epsilon = -\frac{\lambda_{max}(\Xi)}{|I + K_p^\top K_p|}$, with $\Xi := \mathrm{He}\left(\bar{P}_p(A_p + B_p K_p) + \frac{\tilde{\alpha}}{2}\bar{P}_p\right)$. Moreover there exists $K > 0$ such that for all $\xi(t_0,0) = (x(t_0,0), \tau(t_0,0)) \in \mathbb{R}^n \times [0, 2\rho]$, we have

$$
V(x(t,j)) \le \frac{a_1}{a_2} K^2 \exp(-\tilde{\alpha}(t - t_0)) V(x(t_0,0)), \qquad (50)
$$

for all $(t,j) \in \mathrm{dom}(\xi)$, where $a_1 := \lambda_{min}(P)$ and $a_2 := \lambda_{max}(P)$. ◊

Remark 9: Exact bounds. Similar to Theorem 1, $\overline{\rho}$ satisfying conditions of Lemma 2 can be obtained through the following expression:

$$
\overline{\rho} := \varphi_e^{-1}\left(-\frac{\lambda_{max}(\Xi)}{2|MA|(1 + |K_p^\top K_p|)}\right), \qquad (51)
$$

with $\varphi_e(s) := \frac{1}{2|A|}(\exp(2|A|s) - 1)$, A defined in (16) and Ξ defined in the statement.

Moreover Lemma 2 establishes global exponential stability of set $\{0\} \times [0, 2\rho]$ and returns the exponential bound (50), which implies t-decay rate $\tilde{\alpha}/2$. Notice that $\tilde{\alpha} \in (0, \alpha]$ is a design parameter which is selected in the flow and jump sets $\mathcal{F}$ and $\mathcal{J}$ through (15b), with $\alpha > 0$ satisfying (48a). In particular the gain K in (50) can be defined as:

$$
K = \frac{\lambda_{max}(P)}{\lambda_{min}(P)} \exp\left((\tilde{\alpha} + 2|A|)\frac{\rho}{2}\right), \qquad (52)
$$

which takes into account the increase of the Lyapunov function that may occur in the first interval due to the dwell time (see Remark 1 for further details). Indeed bound (50) can be tightened by expressing the dependence of K on $\tau(0,0)$.

Although we preferred to keep the proof of Lemma 2 simple, we can modify the proof technique to replace K in (50) by $\tilde{K}(\tau(0,0))$ defined as

$$\tilde{K}(\tau(0,0)) := \frac{\lambda_{max}(P)}{\lambda_{min}(P)} \exp\left((\tilde{\alpha} + 2|A|)\frac{\max\{0, \rho - \tau(0,0)\}}{2}\right), \tag{53}$$

with $\tau(0,0) \in [0, 2\rho]$. This new $\tilde{K}(\tau(0,0))$ takes into account that whenever $\tau(0,0) \in [\rho, 2\rho]$, system (3)-(4), (16) is ready to jump if $x \notin \mathcal{F}$ and in that case the exponential term in (53) disappears, making the accuracy of bound (50) depend only on the condition number of matrix P (see [5]). Notice that the bound (50) with $\tilde{K}(\tau(0,0))$ instead of K is tighter since $\tilde{K}(\tau(0,0)) \leq K$. ⋆

Proof of Lemma 2. First notice that

$$\lambda_{min}(P)|x|^2 \leq V(x) \leq \lambda_{max}(P)|x|^2, \quad \forall x \in \mathbb{R}^n. \tag{54}$$

Furthermore, we have $\langle \nabla V(x), Ax \rangle = x^\top \mathrm{He}(PA)x$, thus the flow and jump sets defined in (4c) and (4d) by means of M in (15b) can be rewritten as

$$\begin{aligned}
\mathcal{F} &= \{x \in \mathbb{R}^n : x^\top \mathrm{He}\left(PA + \frac{\tilde{\alpha}}{2}P\right)x \leq 0\} \\
&= \{x \in \mathbb{R}^n : \langle \nabla V(x), Ax \rangle + \tilde{\alpha} V(x) \leq 0\}, \qquad (55a) \\
\mathcal{J} &= \{x \in \mathbb{R}^n : x^\top \mathrm{He}\left(PA + \frac{\tilde{\alpha}}{2}P\right)x \geq 0\} \\
&= \{x \in \mathbb{R}^n : \langle \nabla V(x), Ax \rangle + \tilde{\alpha} V(x) \geq 0\}. \qquad (55b)
\end{aligned}$$

Define $V_p(x_p) = x_p^\top \bar{P}_p x_p$, then from the definitions of P, G (see (16)) and (48b), we have $\bar{P}_p = \bar{P}_p^\top > 0$ and

$$\begin{aligned}
V(x^+) &= V(Gx) = x^\top G^\top P G x \\
&= x^\top \begin{bmatrix} I & K_p^\top \\ 0 & 0 \end{bmatrix} \begin{bmatrix} P_p & P_{pc} \\ P_{pc}^\top & P_c \end{bmatrix} \begin{bmatrix} I & 0 \\ K_p & 0 \end{bmatrix} x \\
&= x^\top \begin{bmatrix} P_p + K_p^\top P_{pc}^\top + P_{pc} K_p + K_p^\top P_c K_p & 0 \\ 0 & 0 \end{bmatrix} x \\
&= x_p^\top (P_p + K_p^\top P_{pc}^\top + P_{pc} K_p + K_p^\top P_c K_p) x_p \\
&= x_p^\top \bar{P}_p x_p = V_p(x_p), \qquad (56)
\end{aligned}$$

for all $x \in \mathbb{R}^n$.

Consider the Lyapunov function $x \mapsto V(x)$ at jumps. By using (48b) and (56), we have

$$\begin{aligned}
\Delta V(x) &= V(x^+) - V(x) \\
&= x_p^\top \bar{P}_p x_p - x_p^\top P_p x_p - 2 x_p^\top P_{pc} x_c - x_c^\top P_c x_c \\
&= \begin{bmatrix} x_p \\ x_c \end{bmatrix}^\top \begin{bmatrix} -P_{pc} P_c^{-1} P_{pc}^\top & -P_{pc} \\ -P_{pc}^\top & -P_c \end{bmatrix} \begin{bmatrix} x_p \\ x_c \end{bmatrix} \leq 0,
\end{aligned}$$

for all $x \in \mathbb{R}^n$, where last inequality is obtained by applying a Schur complement (see [4, pag. 28]) and implies (49a).

Now recall that $x = (x_p, x_c)$ and $x^+ = (x_p, K_p x_p)$ and notice that $|Gx|^2 = x_p^\top (I + K_p^\top K_p) x_p \leq |I + K_p^\top K_p| |x_p|^2$. From the definition of $\tilde{\mathcal{F}}$ in the statement (see also (8)), we have $\tilde{M} = M + \epsilon I = \mathrm{He}\left(PA + \frac{\tilde{\alpha}}{2}P\right) + \epsilon I$ and $\tilde{\mathcal{F}}_\epsilon$ defined in (9) accordingly (namely, $\tilde{M} - \epsilon I = M$, that is $\mathcal{F} = \tilde{\mathcal{F}}_\epsilon$) and by noticing that $P_p + K_p^\top P_{pc}^\top = \bar{P}_p$ and $P_{pc} + K_p^\top P_c = 0$, we have

$$\begin{aligned}
x^\top G^\top \tilde{M} G x &= x^\top G^\top (M + \epsilon I) G x \\
&= x^\top \left(\mathrm{He}\left(\begin{bmatrix} \bar{P}_p (A_p + B_p K_p) + \frac{\tilde{\alpha}}{2} \bar{P}_p & 0 \\ 0 & 0 \end{bmatrix} \right) \right. \\
&\qquad \left. + \epsilon \begin{bmatrix} I + K_p^\top K_p & 0 \\ 0 & 0 \end{bmatrix} \right) x \\
&= \begin{bmatrix} x_p \\ x_c \end{bmatrix}^\top \begin{bmatrix} \Xi + \epsilon(I + K_p^\top K_p) & 0 \\ 0 & 0 \end{bmatrix} \begin{bmatrix} x_p \\ x_c \end{bmatrix} \\
&\leq \begin{bmatrix} x_p \\ x_c \end{bmatrix}^\top \begin{bmatrix} (\lambda_{max}(\Xi) + \epsilon |I + K_p^\top K_p|) I & 0 \\ 0 & 0 \end{bmatrix} \begin{bmatrix} x_p \\ x_c \end{bmatrix} \\
&= 0, \quad \forall x \in \mathbb{R}^n, \qquad (57)
\end{aligned}$$

which implies $Gx \in \tilde{\mathcal{F}}$, for all $x \in \mathcal{J}$ and $\tilde{\mathcal{F}} \subset \mathcal{F} = \tilde{\mathcal{F}}_\epsilon$, whenever $\epsilon = -\frac{\lambda_{max}(\Xi)}{|I + K_p^\top K_p|} > 0$. Therefore also condition (49b) is satisfied.

Consider the Lyapunov function $x \mapsto V(x)$ during flow. It is straightforward from (55a) to have

$$\langle \nabla V(x), Ax \rangle \leq -\tilde{\alpha} V(x), \quad \forall x \in \mathcal{F} = \tilde{\mathcal{F}}_\epsilon. \tag{58}$$

Now consider a generic solution ξ with its hybrid time domain $(t, j) \in \mathrm{dom}(\xi)$. Notice that due to the dwell time, we have $t_{i+1} - t_i \geq \rho > 0$, for all $i \in \mathbb{Z}_{\geq 1}$.

By applying Claim 1 there exists $\bar{\rho} > 0$ (see (51)) such that for all $\rho \in (0, \bar{\rho})$, $x(t,i) \in \tilde{\mathcal{F}}_\epsilon$ for all $t \in [t_i, t_{i+1}]$, $i \in \mathbb{Z}_{\geq 1}$. Therefore from (58), we have

$$V(x(t,i)) \leq \exp(-\tilde{\alpha}(t - t_i)) V(x(t_i, i)), \tag{59}$$

for all $t \in [t_i, t_{i+1}]$, $i \in \mathbb{Z}_{\geq 1}$.

Regarding the interval $[t_0, t_1]$, we consider two subcases: $t \in [t_0, t_0 + \rho]$ and $t \in (t_0 + \rho, t_1]$.

Case i: $t \in [t_0, t_0 + \rho]$. From $|\dot{x}| \leq |A||x|$, one has $|x(t,i)|^2 \leq \exp(2|A|(t - t_i))|x(t_i, i)|^2$ for all $t \in [t_i, t_{i+1}]$, $i \in \mathbb{Z}_{\geq 0}$ and so also in the interval of interest. Therefore we get

$$V(x(t,0)) \leq \frac{a_2}{a_1} \exp(2|A|(t - t_0)) V(x(t_0, 0)),$$

where $a_1 := \lambda_{min}(P)$ and $a_2 := \lambda_{max}(P)$.

Case ii: $t \in (t_0 + \rho, t_1]$. By Remark 1 item ii, we have $x(t,0) \in \mathcal{F} = \tilde{\mathcal{F}}_\epsilon$ for all $t \in (t_0 + \rho, t_1]$, therefore also (59) holds.

By combining the two subcases, one has

$$\begin{aligned}
V(x(t,0)) &\leq \exp(-\tilde{\alpha}(t - t_0 - \rho)) V(x(t_0 + \rho, 0)) \\
&\leq \frac{a_2}{a_1} \exp(2|A|\rho) \exp(-\tilde{\alpha}(t - t_0 - \rho)) V(x(t_0, 0)) \\
&= \frac{a_2}{a_1} \exp((2|A| + \tilde{\alpha})\rho) \exp(-\tilde{\alpha}(t - t_0)) V(x(t_0, 0)) \\
&= \frac{a_1}{a_2} K^2 \exp(-\tilde{\alpha}(t - t_0)) V(x(t_0, 0)), \qquad (60)
\end{aligned}$$

for all $t \in [t_0, t_1]$.

Finally, by combining (49a), (59) and (60), we have (50). This concludes the proof of Lemma 2. ■

$$\mathrm{He}\left(\left[\begin{array}{cc|cc} (1-\tau_S)(\bar{A}_pY+\bar{B}_p\hat{C})-\frac{\tau_S\tilde{\alpha}-a_3}{2}Y & (1-\tau_S)(\bar{A}_p+\bar{B}_p\hat{D}\bar{C}_p)-\frac{\tau_S\tilde{\alpha}-a_3}{2}I & \bar{B}_w+\bar{B}_p\hat{D}\bar{D}_w & 0 \\ (1-\tau_S)\hat{A}-\frac{\tau_S\tilde{\alpha}-a_3}{2}I & (1-\tau_S)(W\bar{A}_p+\hat{B}\bar{C}_p)-\frac{\tau_S\tilde{\alpha}-a_3}{2}W & W\bar{B}_w+\hat{B}\bar{D}_w & 0 \\ \hline 0 & 0 & -\frac{\gamma}{2}I & 0 \\ \bar{C}_zY+\bar{D}_z\hat{C} & \bar{C}_z+\bar{D}_z\hat{D}\bar{C}_p & \bar{D}_{zw}+\bar{D}_z\hat{D}\bar{D}_w & -\frac{\gamma}{2}I \end{array}\right]\right)<0, \tag{61}$$

Proof of Theorem 2. The proof is carried out by showing that conditions (19) and definitions (17) imply all the conditions of Lemma 2 and Proposition 1, by using the same Lyapunov function $V(x)=x^\top Px$, with $P=P^\top>0$.

In particular, consider the following partitioned matrix $P=P^\top=\left[\begin{smallmatrix} Y & Z \\ Z & Z\end{smallmatrix}\right]^{-1}>0$. By applying the matrix inversion lemma in [18], we get

$$\begin{aligned} P&=\left[\begin{array}{cc} Y & Z \\ Z & Z\end{array}\right]^{-1}=\left[\begin{array}{cc} (Y-Z)^{-1} & -(Y-Z)^{-1} \\ -(Y-Z)^{-1} & Z^{-1}+(Y-Z)^{-1}\end{array}\right] \\ &:=\left[\begin{array}{cc} W & -W \\ -W & W+Z^{-1}\end{array}\right], \end{aligned} \tag{62}$$

which corresponds to the first of (17) (notice that since $W=(Y-Z)^{-1}$, we have also $Z=Y-W^{-1}$ or equivalently $Y=Z+W^{-1}$). Similarly to [24], [35], by pre- and post-multiplying (62) by $\Pi:=\left[\begin{smallmatrix} Y & Z \\ I & 0\end{smallmatrix}\right]$ (note that $\Pi P=\left[\begin{smallmatrix} I & 0 \\ W & -W\end{smallmatrix}\right]$), and its transpose, we get (19a), which implies $P=P^\top>0$.

By defining $R=W+Z^{-1}$ and by applying again the matrix inversion lemma (see [18]), we can establish the following useful identities

$$\begin{aligned} R^{-1}&=(W+Z^{-1})^{-1}=W^{-1}-W^{-1}(Z+W^{-1})^{-1}W^{-1} \\ &=(Y-Z)-(Y-Z)(Z+(Y-Z))^{-1}(Y-Z) \\ &=(Y-Z)-(Y-Z)Y^{-1}(Y-Z) \\ &=(I-(Y-Z)Y^{-1})(Y-Z) \\ &=(YY^{-1}-(Y-Z)Y^{-1})(Y-Z) \\ &=(Y-(Y-Z))Y^{-1}(Y-Z) \\ &=ZY^{-1}(Y-Z). \end{aligned} \tag{63}$$

Consider also the following definitions

$$\begin{aligned} \hat{A}&:=W(-\bar{A}_cZ-\bar{B}_c\bar{C}_pY+\bar{B}_p\bar{C}_cZ+(\bar{A}_p+\bar{B}_p\bar{D}_c\bar{C}_p)Y), \\ \hat{B}&:=W(-\bar{B}_c+\bar{B}_p\bar{D}_c), \\ \hat{C}&:=\bar{C}_cZ+\bar{D}_c\bar{C}_pY, \\ \hat{D}&:=\bar{D}_c, \end{aligned} \tag{64}$$

and notice that we retrieve (17) from (64) and vice versa.

Let us now show that all the conditions of Lemma 2 are satisfied. By imposing $P=\left[\begin{smallmatrix} P_p & P_{pc} \\ P_{pc}^\top & P_c\end{smallmatrix}\right]=\left[\begin{smallmatrix} W & -W \\ -W & W+Z^{-1}\end{smallmatrix}\right]$ and using (62) and last one in (63), we have

$$\begin{aligned} \bar{P}_p=P_p-P_{pc}P_c^{-1}P_{pc}^\top&=W-W(W+Z^{-1})^{-1}W \\ &=W-WZY^{-1}(Y-Z)W \\ &=W-WZY^{-1}W^{-1}W \\ &=W(I-ZY^{-1}) \\ &=W(Y-Z)Y^{-1} \\ &=WW^{-1}Y^{-1}=Y^{-1}, \end{aligned}$$

which implies the first one of (48b), and

$$\begin{aligned} K_p=-P_c^{-1}P_{pc}^\top&=(W+Z^{-1})^{-1}W \\ &=ZY^{-1}W^{-1}W \\ &=(Y-W^{-1})Y^{-1}, \end{aligned}$$

which returns the second definition in (48b) and the second definition of (17). Furthermore, by multiplying (19b) on both sides by $\bar{P}_p=Y^{-1}$ and using (64) and (62), we get

$$\begin{aligned} \mathrm{He}(Y^{-1}(\bar{A}_p+\bar{B}_p\hat{C}Y^{-1}))+\alpha Y^{-1}&=\mathrm{He}(Y^{-1}(\bar{A}_p \\ &+\bar{B}_p(\bar{C}_c(Y-W^{-1})+\bar{D}_c\bar{C}_pY)Y^{-1}))+\alpha Y^{-1} \\ &=\mathrm{He}(\bar{P}_p(A_p+B_pK_p))+\alpha\bar{P}_p, \end{aligned} \tag{65}$$

from which we get (48a) and therefore Lemma 2 holds and hence also (49).

Notice that from (50) with K in (52) and the fact that $a_1|x|^2\le V(x)\le a_2|x|^2$ with $a_1:=\lambda_{min}(P)$ and $a_2:=\lambda_{max}(P)$, we get

$$|x(t,j)|^2\le K\exp(-\frac{\tilde{\alpha}}{2}(t-t_0))|x(t_0,0)|^2,\quad (t,j)\in\mathrm{dom}(\xi),$$

which returns item i of Definition 1. This completes the proof of the first item of Theorem 2.

We want to prove now that (17) and (19) imply conditions (13), so that Proposition 1 holds. First let us select $M=\tilde{M}-\epsilon I$ (similarly to the proof of Lemma 2) and notice that (13c) is directly satisfied with $\tau_F=1$. Moreover, conditions (49) imply (13b) with $\underline{\rho}=\tau_R=0$ and (13d) with $\tau_C=0$, respectively.

Consider now condition (13a), with P in (62), $\tilde{M}-\epsilon I=M=\mathrm{He}(PA)+\tilde{\alpha}P$. By pre- and post-multiplying (13a) by $T:=\left[\begin{smallmatrix} \Pi & 0 & 0 \\ 0 & I & 0 \\ 0 & 0 & I\end{smallmatrix}\right]$ and its transpose, and by using (64), condition (13a) is equivalent to (61), which is implied by (19c), since $a_3>0$ can be selected a posteriori due to the strict inequality (see Remark 5). Therefore (13) are satisfied, Proposition 1 holds and this completes the proof of item ii and hence of the theorem. ■

VI. Conclusions

The analysis and synthesis for hybrid systems has been presented. The analysis accounts for the t-$\mathcal{L}_2$ gain estimate and it can be applied to a rather wide class of hybrid systems

of interest in the present scientific literature [2], [13], [27], [28]. New relaxed conditions are presented for the analysis with respect to [29].

The synthesis exploits the property of a new reset controller presented in [12]. It presents the advantage to preserve convexity (although with a line search) whenever the flow and jump sets have to be taken into account during the synthesis. This method seems to be much more flexible than the optimization-based synthesis in [10] where a different $\mathcal{H}_\infty$ reset controller architecture was used. The new synthesis allows the design of an $\mathcal{H}_\infty$ reset controller whose continuous-time part does not stabilize the feedback. At the same time the numerical examples seem to suggest that t-$\mathcal{L}_2$ stability is better preserved whenever a hybrid controller with stabilizing continuous-time part is selected.

Further developments might interest the use of this new reset controller architecture to perform optimization-based synthesis with respect to other performance indexes.

REFERENCES

[1] A. Banos, J. Carrasco, and A. Barreiro. Reset Times-Dependent Stability of Reset Control Systems. *IEEE Transactions on Automatic Control*, 56(1):217–223, 2011.

[2] O. Beker, C Hollot, and Y. Chait. Fundamental Properties of Reset Control Systems. *Automatica*, 40(6):905–915, 2004.

[3] O. Beker, C.V. Hollot, and Y. Chait. Plant with an Integrator: an Example of Reset Control Overcoming Limitations of Linear Feedback. *IEEE Transactions on Automatic Control*, 46(11):1797–1799, November 2001.

[4] S.P. Boyd, L. El Ghaoui, E. Feron, and V. Balakrishnan. *Linear Matrix Inequalities in System and Control Theory.* Society for Industrial and Applied Mathematics, 1994.

[5] R.L. Burden and J.D. Faires. *Numerical Analysis.* Thomson Brooks/Cole, 2005.

[6] C. Cai and A.R. Teel. Characterizations of Input-to-state Stability for Hybrid Systems. *Systems & Control Letters*, 58(1):47–53, 2009.

[7] C. Cai, A.R. Teel, and R. Goebel. Smooth Lyapunov Functions for Hybrid Systems, Part II: (Pre)Asymptotically Stable Compact Sets. *IEEE Transactions on Automatic Control*, 53(3):734–748, 2008.

[8] Q. Chen, Y. Chait, and C.V. Hollot. Analysis of Reset Control Systems Consisting of a FORE and Second Order Loop. *J. Dynamic Systems, Measurement and Control*, 123:279–283, 2001.

[9] M. Chilali and P. Gahinet. H_∞ Design with Pole Placement Constraints: an LMI Approach. *IEEE Transactions on Automatic Control*, 41:358–367, 1996.

[10] F. Fichera, C. Prieur, S. Tarbouriech, and L. Zaccarian. A Convex Hybrid $\mathcal{H}_\infty$ Synthesis with Guaranteed Convergence Rate. In *Proceedings of the 51st Conference on Decision and Control*, pages 4217–4222, Maui (HI), USA, 2012.

[11] F. Fichera, C. Prieur, S. Tarbouriech, and L. Zaccarian. Improving the Performance of Linear Systems by Adding a Hybrid Loop: the Output Feedback Case. In *Proceedings of the 2012 American Control Conference*, pages 3192–3197, Montreal, Canada, 2012.

[12] F. Fichera, C. Prieur, S. Tarbouriech, and L. Zaccarian. On Hybrid State-feedback Loops Based on a Dwell-time Logic. In *4th IFAC Conference on Analysis and Design of Hybrid Systems*, pages 388–393, Eindhoven, The Netherlands, 2012.

[13] F. Fichera, C. Prieur, S. Tarbouriech, and L. Zaccarian. Using Luenberger Observers and Dwell-time Logic for Feedback Hybrid Loops in Continuous-time Control Systems. *International Journal of Robust and Nonlinear Control*, 23:1065–1086, 2013.

[14] F. Forni, D. Nešić, and L. Zaccarian. Reset Passivation of Nonlinear Controllers via Suitable Time-regular Reset Map. *Automatica*, 47(9):2099–2106, 2011.

[15] R. Goebel, R.G. Sanfelice, and A.R. Teel. Hybrid Dynamical Systems. *IEEE Control Systems Magazine*, 29(2):28–93, April 2009.

[16] R. Goebel, R.G. Sanfelice, and A.R. Teel. *Hybrid Dynamical Systems: Modeling, Stability and Robustness.* Princeton University Press, 2012.

[17] R. Goebel and A.R. Teel. Direct Design of Robustly Asymptotically Stabilizing Hybrid Feedback. *ESAIM: Control Optim. Calc. Var.*, 15(1):205–213, 2009.

[18] G.H. Golub and C.F. Van Loan. *Matrix Computations*, volume 3. Johns Hopkins University Press, 2012.

[19] J.P. Hespanha, D. Liberzon, and A.S. Morse. Hysteresis-based Switching Algorithms for Supervisory. *Automatica*, 39(2):263–272, 2004.

[20] P. Kapasouris, M. Athans, and G. Stein. Design of Feedback Control Systems for Stable Plants with Saturating Actuators. In *Proceedings of the 27th IEEE Conference on Decision and Control*, pages 469–479, Austin, TX, 1988.

[21] H.K. Khalil. *Nonlinear Systems.* Prentice Hall, PTR, 2002.

[22] J. Löfberg. YALMIP : A Toolbox for Modeling and Optimization in MATLAB. In *Proceedings of the CACSD Conference*, Taipei, Taiwan, 2004.

[23] D.G. Luenberger. Observers for Multivariable Systems. *IEEE Transactions on Automatic Control*, 11(2):190–197, 1966.

[24] I. Masubuchi, A. Ohara, and N. Suda. LMI-based Controller Synthesis: a Unified Formulation and Solution. *International Journal of Robust and Nonlinear Control*, 8(8):669–686, 1998.

[25] H. Neudecker. A Note on Kronecker Matrix Products and Matrix Equation Systems. *SIAM Journal on Applied Mathematics*, 17(3):603–606, 1969.

[26] D. Nešić, A.R. Teel, G. Valmorbida, and L. Zaccarian. Finite-Gain $\mathcal{L}_p$ Stability for Hybrid Dynamical Systems. *Automatica*, 2013, on-line.

[27] D. Nešić, A.R. Teel, and L. Zaccarian. Stability and Performance of SISO Control Systems with First Order Reset Elements. *IEEE Transactions on Automatic Control*, 56(11):2567–2582, 2011.

[28] D. Nešić, L. Zaccarian, and A.R. Teel. Stability Properties of Reset Systems. In *Proceedings of the 16th IFAC World Congress*, pages 67–72, Prague, Czech Republic, 2005.

[29] D. Nešić, L. Zaccarian, and A.R. Teel. Stability Properties of Reset Systems. *Automatica*, 44(8):2019–2026, 2008.

[30] C. Prieur and A. Astolfi. Robust Stabilization of Chained Systems via Hybrid Control. *IEEE Transactions on Automatic Control*, 48(10):1768–1772, 2003.

[31] C. Prieur, S. Tarbouriech, and L. Zaccarian. Guaranteed Stability for Nonlinear Systems by Means of a Hybrid Loop. In *Proceedings of the 8th IFAC Symposium on Nonlinear Control Systems (NOLCOS)*, pages 72–77, Bologna, Italy, September 2010.

[32] C. Prieur, S. Tarbouriech, and L. Zaccarian. Improving the Performance of Linear Systems by adding a Hybrid Loop. In *18th IFAC World Congress*, pages 6301–6306, Milano, Italy, September 2011.

[33] C. Prieur, S. Tarbouriech, and L. Zaccarian. Lyapunov-based hybrid loops for stability and performance of continuous-time control systems. *Automatica*, 49(2):577–584, 2013.

[34] A. Satoh. State Feedback Synthesis of Linear Reset Control with $\mathcal{L}_2$ Performance Bound via LMI Approach. In *IFAC 18th World Congress*, pages 5860–5865, Milan, Italy, 2011.

[35] C. Scherer, P. Gahinet, and M. Chilali. Multiobjective Output-feedback Control via LMI Optimization. *IEEE Transactions on Automatic Control*, 42(7):896–911, 1997.

[36] A.R. Teel, F. Forni, and L. Zaccarian. Lyapunov-based Sufficient Conditions for Exponential Stability in Hybrid Systems. *IEEE Transactions on Automatic Control*, 2013, on-line.

[37] L. Zaccarian, D. Nešić, and A.R. Teel. First Order Reset Elements and the Clegg Integrator Revisited. In *Proceedings of the 2005 American Control Conference*, pages 563–568, vol. 1, Portland (OR), USA, June 2005.

[38] L. Zaccarian, D. Nešić, and A.R. Teel. Analytical and Numerical Lyapunov Functions for SISO Linear Control Systems with First-order Reset Elements. *International Journal of Robust and Nonlinear Control*, 21:1134–1158, 2011.